NASA CONTRACTOR
REPORT

Report No. 61290

CHARACTERISTICS AND PROCESSING OF FPS-16/JIMSPHERE RAW RADAR DATA

By R. E. DeMandel and S. J. Krivo
Lockheed Missiles and Space Company
Huntsville Research and Engineering Center
4800 Bradford Blvd.,
Huntsville, Alabama

May 1969

Prepared for

NASA-GEORGE C. MARSHALL SPACE FLIGHT CENTER
Marshall Space Flight center, Alabama 35812

TECHNICAL REPORT STANDARD TITLE PAGE

1. REPORT NO.	2. GOVERNMENT ACCESSION NO.	3. RECIPIENT'S CATALOG NO.
NASA CR-61290		

4. TITLE AND SUBTITLE
CHARACTERISTICS AND PROCESSING OF FPS-16/JIMSPHERE RAW RADAR DATA

5. REPORT DATE
May 1969

6. PERFORMING ORGANIZATION CODE

7. AUTHOR(S)
R. E. DeMandel and S. J. Krivo

8. PERFORMING ORGANIZATION REPORT #
TM 54/50-126

9. PERFORMING ORGANIZATION NAME AND ADDRESS
Lockheed Missiles and Space Company
Huntsville Research & Engineering Center
4800 Bradford Blvd., Huntsville, Alabama

10. WORK UNIT NO.

11. CONTRACT OR GRANT NO.
NAS8-20082

12. SPONSORING AGENCY NAME AND ADDRESS
NASA-Marshall Space Flight Center
Aero-Astrodynamics Laboratory
Marshall Space Flight Center, Alabama

13. TYPE OF REPORT & PERIOD COVERED
NASA Contractor Report

14. SPONSORING AGENCY CODE

15. SUPPLEMENTARY NOTES This work was done under the technical monitorship of Dr. George W. Fichtl, Aerospace Environment Division, NASA-Marshall Space Flight Center.

16. ABSTRACT

The characteristics of FPS-16/Jimsphere raw radar measurements are illustrated and discussed. Errors in these measurements, resulting from faulty data processing, aerodynamic balloon motions and radar performance, are evaluated in terms of their effect upon the accuracy of computed 25-meter wind values.* Wind errors resulting from aerodynamic motions are shown to be insignificant. Stray points and data shifts, which are thought to be incurred during preprocessing of radar tapes, are not always removed by NASA's present editing method and may cause significant errors in computed winds. Slow radar response to changes in the position of the balloon, coupled with the effect of aliasing when 0.1-second radar measurements are converted to 25-meter wind values, may also cause significant errors in computed winds. Recommendations are made, directed toward preventing and eliminating significant types of error.

*The basic data used in this analysis were tabulated at 25-meter intervals; however, the data reduction scheme produced wind velocity values averaged over 50-meter layers. Therefore, all statements about accuracy and similar interpretations of the 25-meter data are with reference to the actual 50-meter layer average winds.

17. KEY WORDS

18. DISTRIBUTION STATEMENT
FOR PUBLIC RELEASE:

E. D. Geissler, Dir, Aero-Astrodynamics Lab
Marshall Space Flight Center

19. SECURITY CLASSIF. (of this report)	20. SECURITY CLASSIF. (of this page)	21. NO. OF PAGES	22. PRICE
U	U	65	

MSFC - Form 3292 (May 1969)

FOREWORD

This document presents the results of work performed by Lockheed's Huntsville Research & Engineering Center while under subcontract to Northrop Nortronics (NSL PO 5-09287) for Marshall Space Flight Center (MSFC) Contract NAS8-20082. This task was conducted in response to the requirement of Appendix A-1, Schedule Order No. 26.

The NASA contract monitor is George Fichtl of the Aerospace Environment Division, Aero-Astrodynamics Laboratory, Marshall Space Flight Center, Alabama.

SUMMARY

The characteristics of FPS-16/Jimsphere raw radar measurements are illustrated and discussed. Errors in these measurements, resulting from faulty data processing, aerodynamic balloon motions and radar performance, are evaluated in terms of their effect upon the accuracy of computed 25-meter wind values. Wind errors resulting from aerodynamic balloon motions are shown to be insignificant. Stray points and data shifts, which are thought to be incurred during preprocessing of radar tapes, are not always removed by NASA's present editing method and may cause significant errors in computed winds. Slow radar response to changes in the position of the balloon, coupled with the effect of aliasing when 0.1-second radar measurements are converted to 25-meter wind values, may also cause significant errors in computed winds. Recommendations are made, directed toward preventing and eliminating significant types of error.

CONTENTS

LIST OF ILLUSTRATIONS

LIST OF ILLUSTRATIONS (Continued)

LIST OF ILLUSTRATIONS (Continued)

Section 1
INTRODUCTION

The FPS-16 radar/Jimsphere precision wind measuring system provides detailed measurements of winds between the earth's surface and 18 km. These measurements constitute a significant improvement over those of former wind measuring systems (Ref. 1), and have been indispensable in the development of space vehicle environmental design, launch and flight criteria. Recently, several investigators have been studying the possibility of increasing the capabilities of this measuring system. Their efforts have been aimed at increasing the accuracy and vertical resolution of FPS-16 radar/Jimsphere measurements so that still smaller wind features, including turbulent fluctuations and vertical motions, can be detected and analyzed.

While the Jimsphere was being developed, extensive research was performed on response and aerodynamic characteristics of various balloon configurations. Because of the thoroughness with which these and subsequent studies were performed, the greatest potential for improvement appears to lie in the areas of radar performance and data processing rather than in sensor design. Indeed, there is much evidence to indicate that important advances can be achieved by upgrading radar operational techniques and modifying existing data-processing procedures.

The objectives of this report are to:

- Familiarize the reader with the characteristics of FPS-16 raw radar data;
- Illustrate the most common types of error found in these data;
- Show the extent to which errors in the 0.1-sec raw radar measurements are removed by editing and their effect on the accuracy of computed 25-m winds; and
- Suggest methods whereby the errors might be prevented at their source or more effectively eliminated by data processing.

Section 2
DISCUSSION

2.1 INTRODUCTION

In Section 2.2 basic features of the FPS-16 radar/Jimsphere system are outlined, and the data processing used by NASA to compute winds at 25-m altitude increments from radar measurements is discussed in Section 2.3. If the reader is familiar with the measuring system and data-processing procedures, he may wish to skip these sections.

The brief discussion of the characteristics of radar data as they are received by NASA/MSFC (Section 2.4) points out the nonstationarity of these measurements and shows some of the anomalies that require that the data be edited before winds are computed. In Section 2.5 several 100-sec sequences of edited radar measurements are discussed in order to illustrate: (1) the fine-scale characteristics of the radar measurements; (2) the fact that bad data are not always eliminated by routine editing; and (3) how features in the radar measurements (range, azimuth and elevation angles) affect computed 0.1-sec values of x, y, z, (position coordinates in the east-west, north-south, and vertical directions, respectively) and u, v, w (velocity values in the x, y, and z directions, respectively). Section 2.6 uses hypothetical examples which closely approximate situations encountered in the radar data to show the effect that selected error types in the 0.1-sec radar measurements have on the accuracy of computed 25-m wind values.

2.2 THE WIND MEASURING SYSTEM

2.2.1 The Sensor

The Jimsphere balloon is a 2-m diameter, rigid, roughened sphere. An internal superpressure of about 5 mb is maintained by two spring-loaded

plastic pressure relief valves. This ensures that the balloon maintains its sphericity at a constant volume. The average mass of a Jimsphere (including 100 g of ballast used to decrease rotation and improve aerodynamic stability) is about 408 g (Ref. 2). The balloon has 398 conical roughness elements, each of which is approximately 3 in. wide at the base and 3 in. high, which serve to control vortex shedding in the supercritical Reynolds number region below 11 km, thereby reducing the magnitude and spectral bandwidth of aerodynamically-induced balloon motions. The Jimsphere is constructed of 1/2 mil aluminized mylar and is a passive target for the AN/FPS-16 radar.

2.2.2 The Radar

The AN/FPS-16 is a high-precision, C-band, monopulse tracking radar, which measures the spherical coordinates of the balloon's position (i.e., range, azimuth angle and elevation angle) at 0.1-sec time intervals. Digital output of time, azimuth, elevation and range ("TAER" data) is recorded on magnetic tape in binary form, with 17 bits (0.002746 deg/bit) for angle measurements and 20 bits (1 yd/bit) for range.

2.3 DATA ACQUISITION AND PROCESSING

2.3.1 Tracking

The radar locks onto the Jimsphere soon after it is released — usually before the balloon reaches an altitude of a few-hundred meters. The balloon is then automatically tracked to at least 17-km altitude unless a malfunction occurs. Between the surface and 17 km, the Jimsphere's ascent rate averages about 4.75 m/sec. Thus, the duration of a typical flight is on the order of one hour.

In addition to the TAER measurements, various radar control settings, events, and operators' observations are recorded. These additional records are useful for investigating accuracy, since the accuracy of the TAER data

is affected by weather conditions, radar performance, manual adjustments made by the operators and by the characteristics of the balloon. Some of these factors are mentioned in Sections 2.4 and 2.5.

2.3.2 Preprocessing

At Patrick Air Force Base, tapes generated at the radar site are converted to a format suitable for machine computation. The converted TAER tapes are then sent to Marshall Space Flight Center where they are subjected to the NASA-developed editing and wind computation procedures.

2.3.3 Editing

Before winds can be computed from the TAER measurements, the data must be edited to correct such irregularities as stray (values which are inconsistent with surrounding data) or missing points which may be incurred during tracking or preprocessing.

Editing consists of generating least-squares, linear fits to sets of nine consecutive values of range, azimuth, and elevation angle. In each case, the center point is then differenced with the fitted value. If the residual exceeds 0.03 deg for azimuth or elevation, or 15 yd* for range, the center point is replaced by the average value over the interval.

To prevent stray points from being included in the computation of the least-squares line, the point immediately following the nine points used in the curve fit is differenced with its corresponding value extrapolated from the fitted line. If the difference exceeds 0.15 deg (or 100 yd for range measurements), the point is rejected and replaced by the extrapolated value. The nine-point interval is then advanced one point, and this procedure is repeated until all the data have been edited. If ten consecutive lead points are

*These numbers represent 3σ values based on an assumed rms error of 0.01 deg for angular measurements and 5 yd for range measurements.

rejected, the program is reinitialized and started again at the point where this occurred.

2.3.4 Computation of Wind*

After the data are edited, the following operations are performed in the sequence listed to provide wind values at altitude increments of 25 m:

1. Convert the 0.1-sec range values from yards to meters and the angle measurements from degrees to radians.
2. Transform the 0.1-sec TAER position points to corresponding 0.1-sec x y z position coordinates.
3. Correct the 0.1-sec x y z points for the effect of the earth's curvature.
4. Combine groups of forty-one 0.1-sec points to produce average values of x y z, at time t, for 25-m increments of altitude. (The first group of 41 consecutive altitude points is selected so that it is approximately centered on an integral multiple of 25 m. A least-squares linear fit to these points is then generated, from which the time, t, corresponding to the desired 25-m level is computed. The corresponding 41-point sets of x and y points are fitted by the same method. The 25-m x and y values are then obtained from their linear functions at time t. The entire process is repeated for each 25-m altitude for which data are available.)
5. Compute the three components of wind velocity by taking centered differences of x y z over 50 m. Scalar wind speed and wind direction are also computed.
6. In a final editing, substitute interpolated values for stray or missing 25-m values.
7. Store the resultant wind data on magnetic tape and on microfilm for future use in engineering and research.

2.4 GROSS FEATURES OF UNEDITED TAER DATA

Radar performance, and consequently the characteristics of radar measurements, vary according to many factors, including atmospheric conditions

*A more thorough treatment of editing and wind computation procedures is presented in Ref. 3.

(wind, clouds, precipitation, etc.), tracking conditions (range, elevation angle, ground clutter, etc.), radar operation (signal-to-noise ratio, servo-bandwidth settings, etc.) and the condition of the radar (calibration, etc.). The statistical characteristics of radar data may vary greatly during an individual flight. This nonstationarity complicates the task of editing and smoothing. The 100-sec sequences of angular measurements shown in Figs. 1 and 2 illustrate the degree to which samples of radar data may differ. The differences in characteristics of these two sequences are almost entirely due to differences in radar performance. The performance and accuracy of the FPS-16 radar are discussed in considerable detail in Refs. 4 through 6.

Serious errors are frequently produced during the preprocessing of radar tapes. Bit-dropping, the most common problem, results in stray points which must be removed before winds are computed. Stray points may be isolated values, as in Fig. 3, or they may appear in groups or even periodically as in Figs. 4 and 5, respectively. Other errors include overlapping (i.e., repeating) segments of data (Fig. 6), missing points, and timing errors. Anomalies like those shown in Figs. 3 through 6 are effectively removed by NASA's editing procedure. Smaller errors, however, are not always removed by the procedure, as is shown in Section 2.5.

2.5 CHARACTERISTICS OF EDITED 0.1-SEC DATA

The following discussion of the fine structure of radar data uses six figures (Figs. 7 through 12) to illustrate typical features of edited FPS-16 radar/Jimsphere measurements. Each figure consists of six sets, labeled (a) through (f), of three component plots. The six sets of plots in each figure are presented in the following sequence:

The first set (a) depicts the variation of elevation angle, range, and azimuth angle for a time interval of 100 sec (i.e., 1000 data points). The second set (b) shows the residuals of elevation angle, range, and azimuth angle after the trend (approximated by a least-squares, seventh-degree

polynomial) has been subtracted from the values shown in (a). This technique is used here to reduce the range of parameter values to permit examination of the small-scale features of the data. It should be pointed out that the large-amplitude, low frequency variations which sometimes appear in the time plots of detrended values (as in the azimuth residuals of Fig. 10b) are probably not real, and reflect, instead, irregularities in the detrending process. The third set (c) presents time plots of x, y and z computed from the radar measurements shown in (a). The fourth set (d) shows the residuals of x, y and z after detrending as described above. The fifth set (e) depicts 0.1-sec velocity values computed from centered differences of the residuals shown in (d) over 0.2-sec intervals. Asterisks indicate points which exceed scale limits. These plots are provided to illustrate the high noise level in unsmoothed radar wind measurements. The sixth set (f) shows spectra of 0.1-sec wind values, computed as described above except that the total wind was used rather than the detrended values in (e). Spectra were computed using the "fast-Fourier transform" method. The spectral values were left unsmoothed to reveal the narrow bandwidth of certain spectral peaks. The first point on each spectrum (corresponding to zero frequency) is indicated by an asterisk. Points which fall below the lower limit of the grid are plotted at the lower limit.

The 100-sec segments of data presented in Figs. 7 through 12 are taken from Test No. 8920, 1400Z, 23 December 1964 at Cape Kennedy, Florida. This ascent was simultaneously tracked by two radars. Data shown in Figs. 7, 9, and 11 were recorded by one of the radars and those in Figs. 8, 10 and 12 were recorded by the other. These figures illustrate important properties of edited radar measurements and their associated errors, and are discussed in Sections 2.5.1 through 2.5.5.

2.5.1 Aerodynamically-Induced Balloon Motions

Between the earth's surface and 11 - 13 km the rising Jimsphere experiences supercritical Reynolds numbers, and the resultant vortex shedding induces a periodic oscillation in the balloon's motion (see Fig. 7b). The oscillation essentially consists of horizontal motions (Fig. 7d). The

aerodynamic balloon motions are very regular, having a frequency of about 0.21 Hz, as revealed by the sharp peaks in the u and v spectra at this frequency (Fig. 7f). The aerodynamic motions tend to damp gradually with altitude and disappear at about 12 km where Reynolds numbers become subcritical. A slight shift toward higher frequency with altitude is also observed. The variation with altitude is revealed by comparing the spectral peaks in Fig. 7f, corresponding to about 1.5 km altitude, with Fig. 8f (about 5.8 km) and Fig. 9f (about 15.5 km).

2.5.2 Noise

The term "noise" refers to high-frequency, random oscillations in the data. Generally, noise increases with the range of the balloon and may be particularly intense when the balloon is being tracked at very low elevation angles, where multipath effects and ground clutter may be pronounced. The characteristics of radar noise are also dependent upon radar control settings – particularly the servo-bandwidth setting (Ref. 7). High bandwidth settings allow high frequency noise while lower settings tend to smooth higher frequencies and shift error into the lower frequencies. Shifting error into lower frequencies is undesirable since it becomes more difficult to filter out error without also losing real wind variations. Hence, servo-bandwidth settings should be maintained as high as possible. As an example of varying noise levels, compare the u, v and w plots of Fig. 7e with those of Fig. 9e. This difference is also reflected in the corresponding spectra (Figs. 7f and 9f). It should be noted that even such "clean" data, as displayed in Fig. 7e, are too noisy for most meteorological applications. This points out the necessity of smoothing the 0.1-sec radar data.

A sharp peak is found at 4 Hz in several of the spectra shown in Figs. 8f, 10f, and 12f. (These data were measured by one radar while the data of Figs. 7, 9, and 11 (where such spectral peaks are absent) were measured by a second radar.) Miers and Avara (Ref. 8) observed a peak at about 4 Hz in spectra of AN/FPS-16 radar slant-range measurements. Four-hertz

peaks were also observed by Jacobs (Ref. 9) in the spectra of angle measurements of another AN/FPS-16 radar. These investigators attributed such peaks to the antenna drive mechanism of the radar.

2.5.3 Stray Points

Although editing does remove extreme-valued stray points, it does not remove all stray values. Some stray points do not deviate enough from the surrounding data to be detected by editing. For example, in the elevation angle residuals shown in Fig. 10b, a cluster of three stray points appears at about 2664.5 sec, and isolated stray values occur at about 2681 sec, 2717.5 sec, and probably at 2743.5 sec. Again, these are considered "stray" values because they appear to be inconsistent with the surrounding data, and are thought to result from bit-dropping when radar tapes are preprocessed. Figs. 10b, 10d, and 10e show how small stray values in elevation angle produce large errors in one or more of the 0.1-sec wind components.

2.5.4 Data Shift

A data shift is defined as a series of consecutive points that are displaced from the trend in the surrounding data by a fixed amount. The shift may be incurred during radar tracking, or it may result from a bit being dropped from each of the consecutive points as the data are preprocessed. The range data shown in Figs. 11a and 11b contain a shift which spans about 70 points between 705 and 712 sec elapsed time. As with the stray points mentioned above, the magnitude of the displacement of those 70 points was too small to cause rejection by the editing routine. Figure 11d shows the effect of this shift on the computed xyz coordinates. The shifts in the xyz position coordinates produce pairs of oppositely directed "stray" values when 0.1-sec wind components are computed (Fig. 11e).

The preceding discussion leads to an important observation regarding the editing of radar data; namely, that editing should be more effective when

it is performed on TAER measurements than on computed 0.1-sec xyz values. Figures 10 and 11 show how an anomaly in one TAER component is transmitted, in varying degree, to each of the computed xyz components. While an anomaly (such as a stray point or shift) may meet the criteria for rejection in its original (TAER component) form, it may not affect one or more of the xyz components enough to meet their rejection criteria. When this happens, part of the error will be retained in the data. Thus, it is more effective to edit the TAER measurements where errors are easier to detect.

Undoubtedly, improved editing techniques can be developed. For example, Zartarian and Thompson (Ref. 10) describe a method developed by the University of Dayton Research Institute where the rejection criteria vary as a function of the standard deviation of preceding data segments. This approach holds promise since it allows for the nonstationarity of FPS-16 radar measurements.* Regardless of the basic editing method used, however, the selection of proper rejection criteria is crucial. Ideally, an editing routine should replace even the smallest stray errors and retain all deviations resulting from ordinary noise (the latter are best removed by filtering). Reference 11 shows that rejection of too many points may reduce the accuracy of the data. The relative effectiveness of various editing procedures and rejection criteria could be tested empirically by using a number of dual tracks (cases in which a balloon is simultaneously tracked by two radars). The better method would produce a lower rms difference between the two sets of computed winds. (This method requires that all other phases of data processing be identical for all cases.)

2.5.5 Radar Response

Radar measurements sometimes reveal a reluctance of the radar to adjust to small angular displacements of the target. The radar antenna

*The UDRI method, however, edits computed values of xyz rather than TAER values.

appears to remain in a fixed position for up to several seconds followed by a rapid correction or over-correction. An example of a large response lag is illustrated in Fig. 2. The elevation angle measurements of Fig. 12a also reveal this type of behavior. Presumably, this lag is associated with the low bandwidth settings which are often used when the balloon is tracked at long range. Radar response lag produces spikes in 0.1-sec component velocity data (Figs. 8e and 12e). In Section 2.6.4 it is shown that radar lag can cause significant errors in 25-m wind data.

2.6 EFFECT OF TAER ERRORS ON COMPUTED 25-M WINDS

To assess the importance of the types of error described above, their effect on the final 25-m wind outputs must be determined. Hypothetical cases that closely resemble observations are used for this purpose.

2.6.1 Aerodynamically-Induced Balloon Motions

The amplitude of the aerodynamic balloon oscillation is about 2 m and its frequency is about 0.21 Hz (Figs. 7d and 7f). The 41-point least-squares linear fit, which has essentially the same effect as a simple average, reduces the amplitude to about 14 percent of its original value, or about 0.28 m. Therefore, the error of any 25-m position coordinate value is $\epsilon \leq 0.28$ m. For a typical ascent rate (5 m/sec), horizontal velocity obtained from centered differences over 50 m, i.e., $\Delta t = 10$ sec, can have a maximum error of only $2\epsilon / \Delta t = 0.056$ m/sec. It is therefore concluded that aerodynamic balloon motions have a negligible effect upon the accuracy of 25-m component velocity values.

2.6.2 Stray Points

As shown in Section 2.5.3, some lesser stray points are not rejected by the editing procedure. To show their effect on computed 25-m wind component values, consider a hypothetical case in which y is increasing

linearly with time*. Suppose also that one stray value, that deviates by H from the linear trend, occurs during the interval of time considered. If the linear trend is removed, the connected 0.1-sec y values would appear as in Fig. 13a.

If the data in (a) are smoothed with a 41-point running mean, (this has the same effect as the least-squares method) the result will appear as in Fig. 13b. In effect, this process differs from the NASA procedure only in that smoothed values are computed for each 0.1 sec, rather than every 5 sec (i.e., every fiftieth point). The effect of the smoothing is to spread the error over a four-second interval, while reducing its magnitude to H/41.

The solid curve in Fig. 13c shows the velocity trace obtained from the smoothed position values in (b) by consecutive differences over 50 m (10 sec). Note that the effect of the stray point in (a) is spread over a 14-sec (70 m) interval, with an amplitude of H/410. Depending upon the points on the time axis where the 25-m velocity values fall, the error may or may not affect the computed velocity values. The most probable effect is that the 25-m velocity values will form a pattern similar to that indicated by the dashed line in (c). It can be seen from Fig. 13c that no error will occur when the first 25-m point falls between three and four seconds elapsed time.

The amplitude of the perturbation which may be produced in the 25-m values is H/410. Taking into consideration the rejection criteria of the editing procedure used on TAER values, it can be shown that H/410 may reach, or even exceed, 0.1 m/sec. For example, an error of 0.03 deg in azimuth angle at a range of about 78 km produces $H \cong 41$ m. Deviations of this magnitude are of little consequence for most applications of wind data. They may, however, be important for applications requiring great precision, such as the computation of vertical motions. It should be noted that when two or more

*In all of the hypothetical cases presented below, the choice of the y component is arbitrary, and the conclusions are equally valid for x and z.

consecutive stray values occur, as in Fig. 10b, velocity errors increase almost proportionally.

2.6.3 Data Shift

Data shifts can produce significant errors in computed 25-m velocity values. To show this, consider a hypothetical shift of 10 m, spanning a 7-sec time interval (i.e., 70 points) in the 0.1-sec y values. This case approximates the observed shift in z in Fig. 11d. The effects of smoothing and differencing are shown in Fig. 14. The resultant velocity fluctuation spans 21 sec (105 m) with an amplitude of 1 m/sec. The 25-m ascent-rate values computed by NASA's data processing routine from the TAER data shown in Fig. 11a, are shown in Fig. 15. The spikes which appear at about 3.7 - 3.8 km in Fig. 15 were caused by the shift in range shown in Fig. 11a. These results verify those predicted by the hypothetical case, and reveal how a shift may induce major errors into the 25-m velocity components.

2.6.4 Radar Response

The angular response of the radar antenna to changes in balloon position, which is a function of the servo-bandwidth setting and other factors, greatly influences the accuracy of the computed (25-m) velocity components. As the response decreases, the rms error of the computed velocities rapidly increases. To show this, two hypothetical cases are presented. In each case, the balloon is east of the radar and traveling northward at 5 m/sec. In the first case the orientation of the antenna alternately remains fixed for a 3-sec time interval followed by a rapid adjustment. In the second case the orientation remains fixed twice as long. Given these conditions, detrended 0.1-sec y values for the two cases might appear as in Figs. 16a and 17a. Similar behavior was observed in elevation angles in Figs. 8b and 12b and in the corresponding z position coordinates in Figs. 8d and 12d. As in the preceding illustrations, Figs. 16 and 17 show the effects of lag on the smoothed position data and on the computed meridional component, v.

The resultant oscillations in v are solely a result of the periodic movements of the radar antenna. In the two cases shown, a doubling of the radar response period produced a doubling of the period of radar-induced oscillations in the computed 0.1-sec meridional wind component, a fourfold increase in amplitude, and a tenfold increase in variance. Thus, error increases rapidly as the radar response decreases.

The above discussion shows the effect of smoothing and differencing each 0.1-sec position point using NASA's method. In actual practice, however, this is only done for every 50th point (assuming a 5 m/sec ascent rate). Therefore, there is the danger of aliasing high frequencies into lower frequencies. This effect is evident in Figs. 16c and 17c where points, indicated by o's, are drawn for 25-m (5-sec) intervals and connected by a dashed line. An increased period in the 25-m points is observed in both cases. In the first case (Fig. 16) the 3-sec period of the oscillation in the 0.1-sec v values becomes 15-sec (or 75 m) in the 25-m values, and in the second case (Fig. 17) the 6-sec period becomes 30-sec (or 150 m).

The conclusion is reached, therefore, that slow radar response can cause significant errors in 25-m computed velocity components, and that these errors may be aliased into lower frequencies that are more likely to interfere with those of real wind variations. By maintaining the maximum possible servo-bandwidth setting, radar response can possibly be increased. Current investigation shows that the detrimental effects of aliasing can be eliminated by using improved filtering techniques.

Section 3
CONCLUSIONS

Based on the preceding discussion, the following basic conclusions are drawn:

- Even under ideal tracking conditions, raw radar measurements contain excessive noise. If unsmoothed 0.1-sec wind values are computed directly from the radar measurements, physically-unrealistic wind variations are observed. Therefore, at least some smoothing is always required. The nonstationarity of FPS-16 raw radar data considerably complicates the tasks of editing and smoothing.
- As winds are now computed, there is the possibility that high-frequency variations in the data may be aliased into lower frequencies.
- The aerodynamically-induced oscillation of the Jimsphere has no discernible vertical component and spans a very narrow spectral band centered at about 0.21 Hz. Its effect upon the accuracy of the computed 25-m wind component values is minimal.
- Stray points and data shifts are thought to result from bit-dropping during preprocessing. Although the NASA-developed editing procedure removes large errors of these types, it does not remove all of them. Thus, these errors can sometimes produce significant errors in computed 25-m wind component values.
- Radar sensitivity, which is a function of the servo-bandwidth setting and other factors, has an important effect upon the accuracy of computed wind values. Wind errors rapidly increase as radar response decreases.

Section 4
RECOMMENDATIONS

The preceding observations concerning the characteristics of FPS-16 radar/Jimsphere measurements suggest the following approaches for improving the accuracy, and therefore the usefulness, of the Jimsphere wind-measuring system:

1. Prevention: Wherever possible, an attempt to prevent the occurrence of errors at their source should be made. Thus, radar operators should be instructed to maintain the maximum possible servo-bandwidth. This would help to minimize errors that result from poor radar response. Furthermore, all other aspects of radar operation and preparation and release of the balloon should be re-evaluated to determine if other improvements could be made.

Preprocessing of radar tapes is another area in which the incidence of errors might be reduced. According to the operators of the preprocessing equipment, timing errors, bit-dropping and overlapping sequences of data could be reduced or eliminated entirely by using better equipment or by improving the performance of existing equipment.

2. Editing: Assuming that some discontinuities may still occur in any set of radar measurements, editing will be required. The effectiveness of a given editing method is measured by its ability to detect, reject, and replace stray and missing values without affecting values whose deviations result from ordinary noise.

Section 2.5.4 points out that the effectiveness of an editing method can be evaluated empirically by applying it to dual radar measurements. The authors suggest that all available editing methods should be compared in this

manner Based on the results of these comparisons, one method would be selected for use in processing FPS-16/Jimsphere data. Once selected, the basic method could be optimized by testing its effectiveness using various point-rejection and substitution criteria.

3. Smoothing: Smoothing is used to reduce errors associated with noise. The smoothing method now used by NASA is equivalent to simple averaging. Because the transfer function of the averaging has appreciable high-frequency lobes, the danger of aliasing exists when 25-m values are computed.

Lockheed/Huntsville recommends that improved techniques be employed to eliminate the possibility of aliasing. The authors have developed a filter which has a transfer function almost identical to that of the present method for wavelengths of 50 m or greater. The filter has no significant high-frequency lobes, and aliasing is thereby prevented.

Lockheed/Huntsville further recommends that the NASA data processing deck provide an option for varying the filter function for special applications. This could be done by inputting any desired cutoff and termination frequencies into the basic filtering routine. Investigators could then select any frequency band for study.

REFERENCES

1. DeMandel, R.E., and James R. Scoggins, "Mesoscale Wave Motions as Revealed by Improved Wind Profile Measurements," J. Applied Meteor., Vol.6, No.4, August 1967, pp.617-620.

2. Eckstrom, Clinton V., "Theoretical Study and Engineering Development of Jimsphere Wind Sensor," NASA Contract NAS8-11158, the G.T. Schjeldahl Co., Advanced Programs Division, Northfield, Minn., July 1965.

3. Biner, Daniel J., "FPS-16 Spherical Balloon Reduction," Doc. No. 0189, Computer Sciences Corp., Huntsville, Ala., 29 April 1967.

4. Mills, Arthur J., "Instrumentation Radar AN/FPS-16 (XN-2), Final Report," Prepared under Contract BuAer NOas 55-869c for Department of the Navy, Bureau of Aeronautics, by Radio Corporation of America, Moorestown, N.J.

5. Bailey, B.K., "Systems Analysis Technical Memorandum No. 27, Radar 1.16 Accuracy Evaluation," MTP-TM-61-17, Air Force Missile Test Center, Patrick AFB, Fla., 22 December 1961.

6. Hoffman-Heyden, A.E., and E.P. Hall, "Radar 3.16 Accuracy Evaluation," MTC-TDR-63-4, Air Force Missile Test Center, Patrick AFB, Fla., 21 February 1963.

7. Engler, Nicholas A., "Methods of Editing Rose Radar Tracking Data," Proceedings of the Third National Conference on Aerospace Meteorology, published by the American Meteorological Society, 6-9 May 1968, pp. 125-131.

8. Miers, B.T., and E.P. Avara, "Analysis of High-Frequency Components of AN/FPS-16 Radar Data," ECOM-5207, Atmospheric Science Research Office, White Sands Missile Range, N.M., August 1968.

9. Jacobs, D.J., "Data Reduction Methods FPS-16 Radar/Jimsphere," Rpt. D5-15564, The Boeing Company, Huntsville, Ala., 1966.

10. Zartarian, Garabed, and John H. Thompson, "Validity of Detailed Balloon Soundings in Booster Vehicle Design," AFCRL-68-0606, Air Force Cambridge Research Laboratories, Bedford, Mass., October 1968.

11. DeMandel, R.E., and S.J. Krivo, "Capability of the FPS-16 Radar/Jimsphere System for Direct Measurement of Vertical Air Motions," NASA CR-61232, Marshall Space Flight Center, Redstone Arsenal, Huntsville, Ala., June 1968.

FIGURES

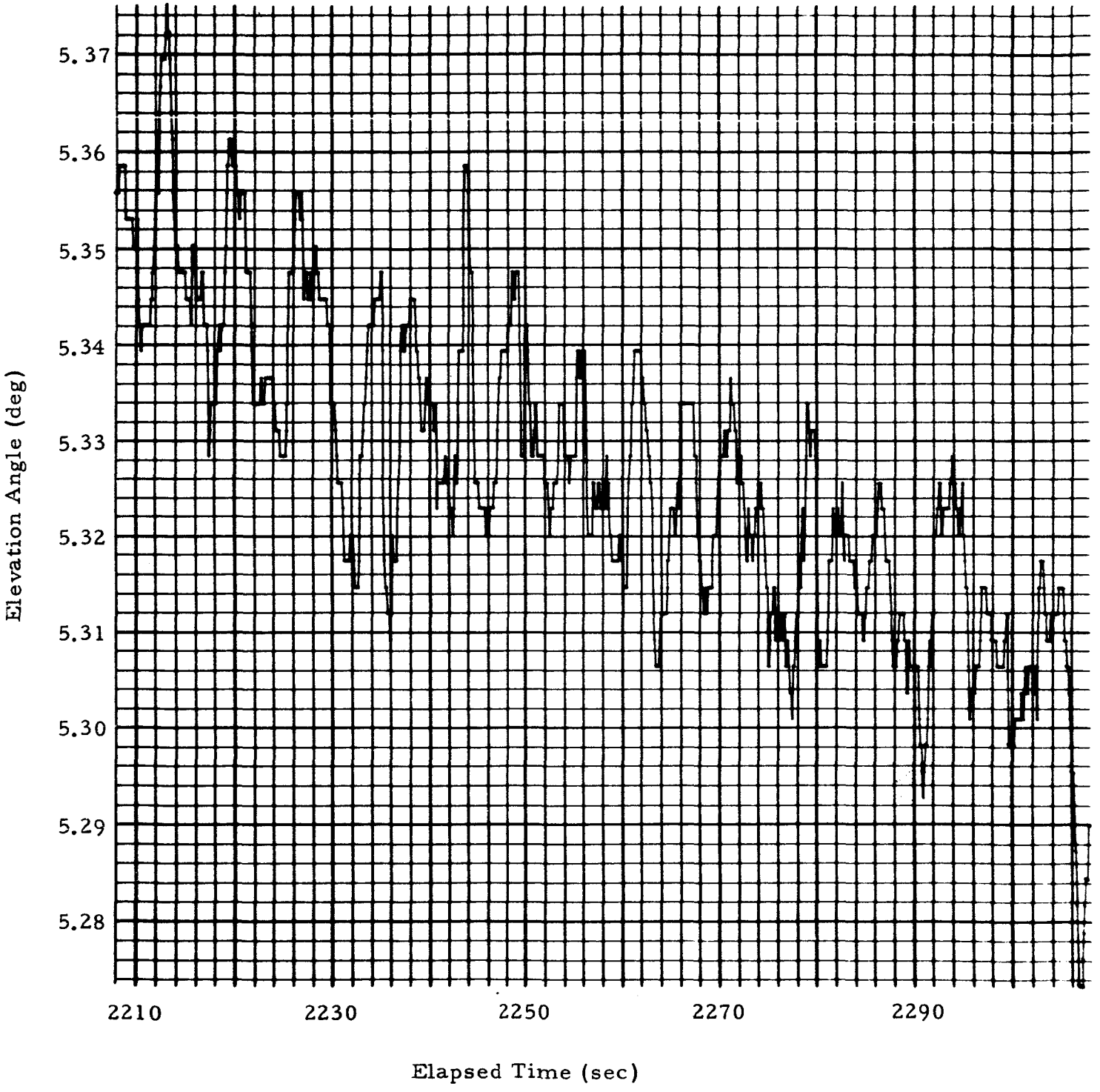

Fig. 1 - Example of Radar Angle Measurements

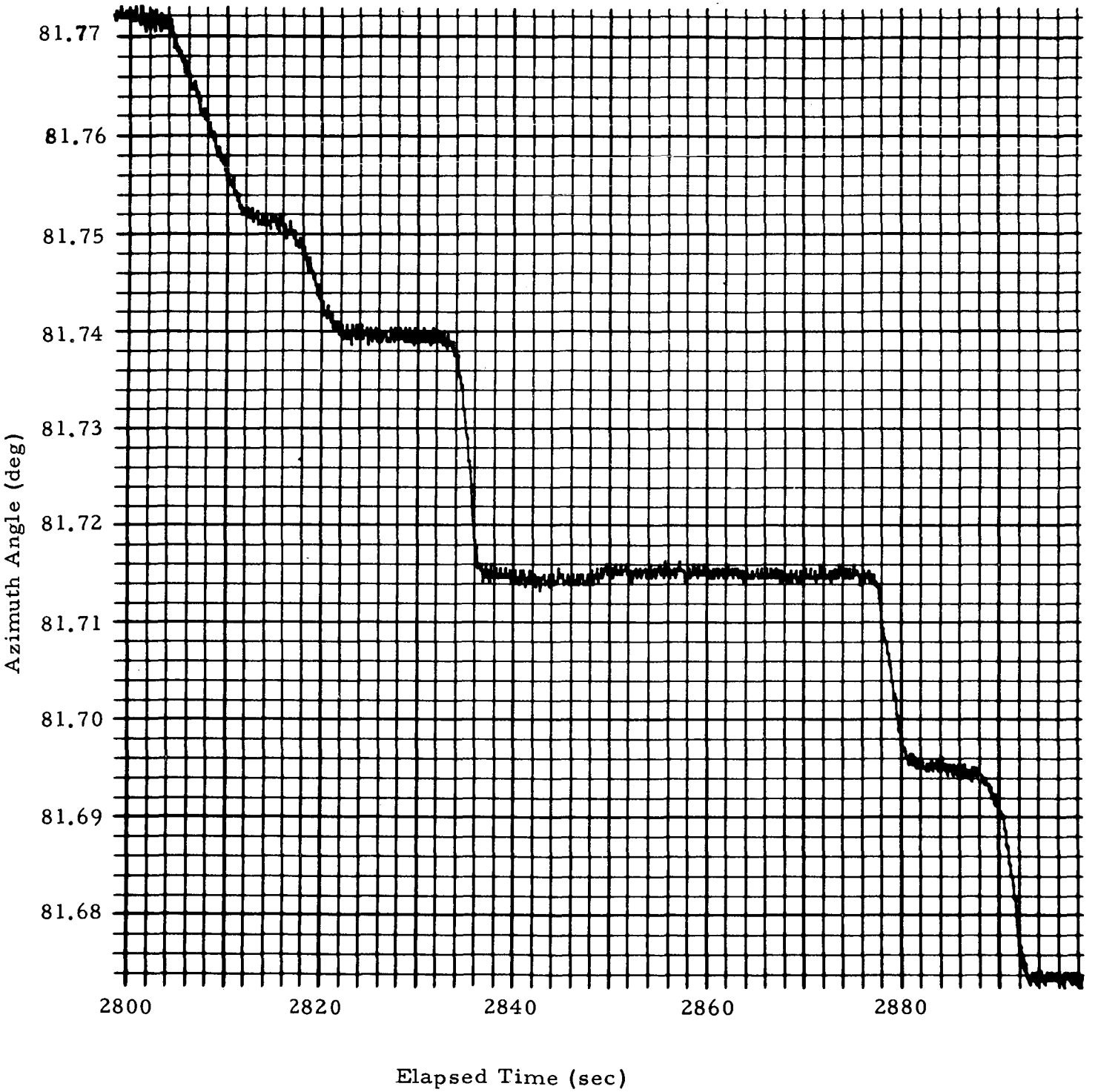

Fig. 2 - Example of Radar Angle Measurements

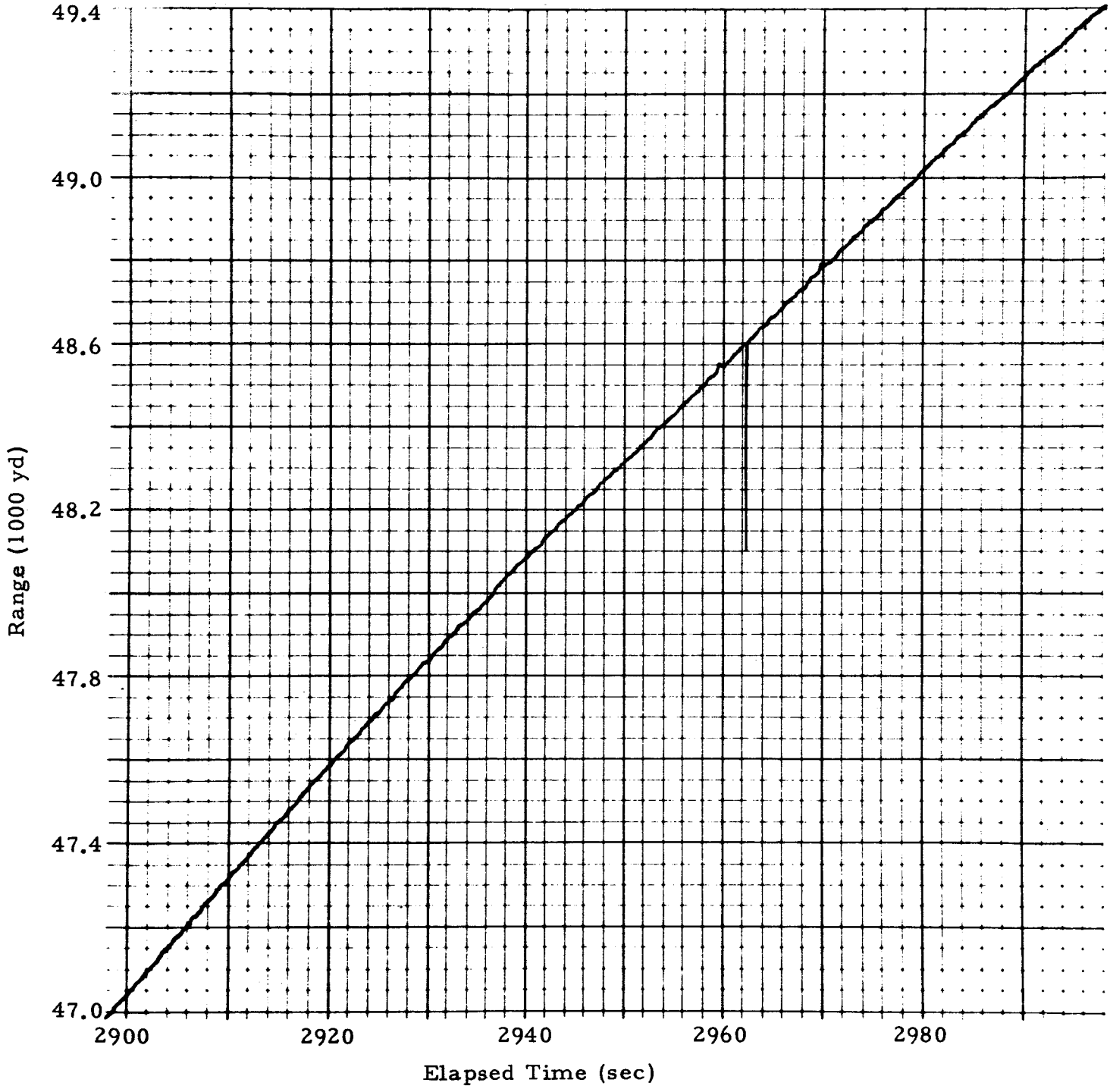

Fig. 3 - Isolated Stray Point

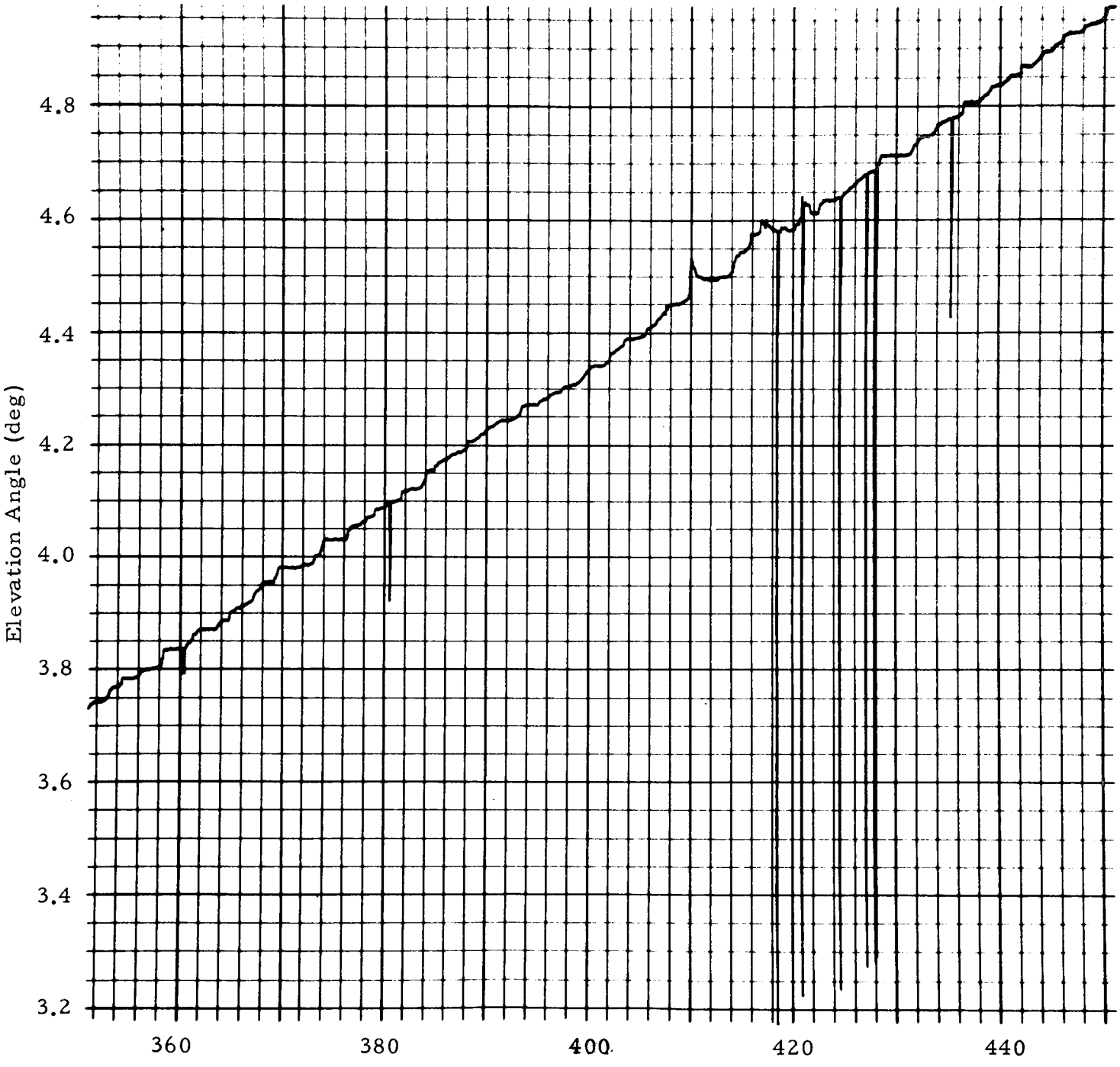

Fig. 4 - Cluster of Stray Points

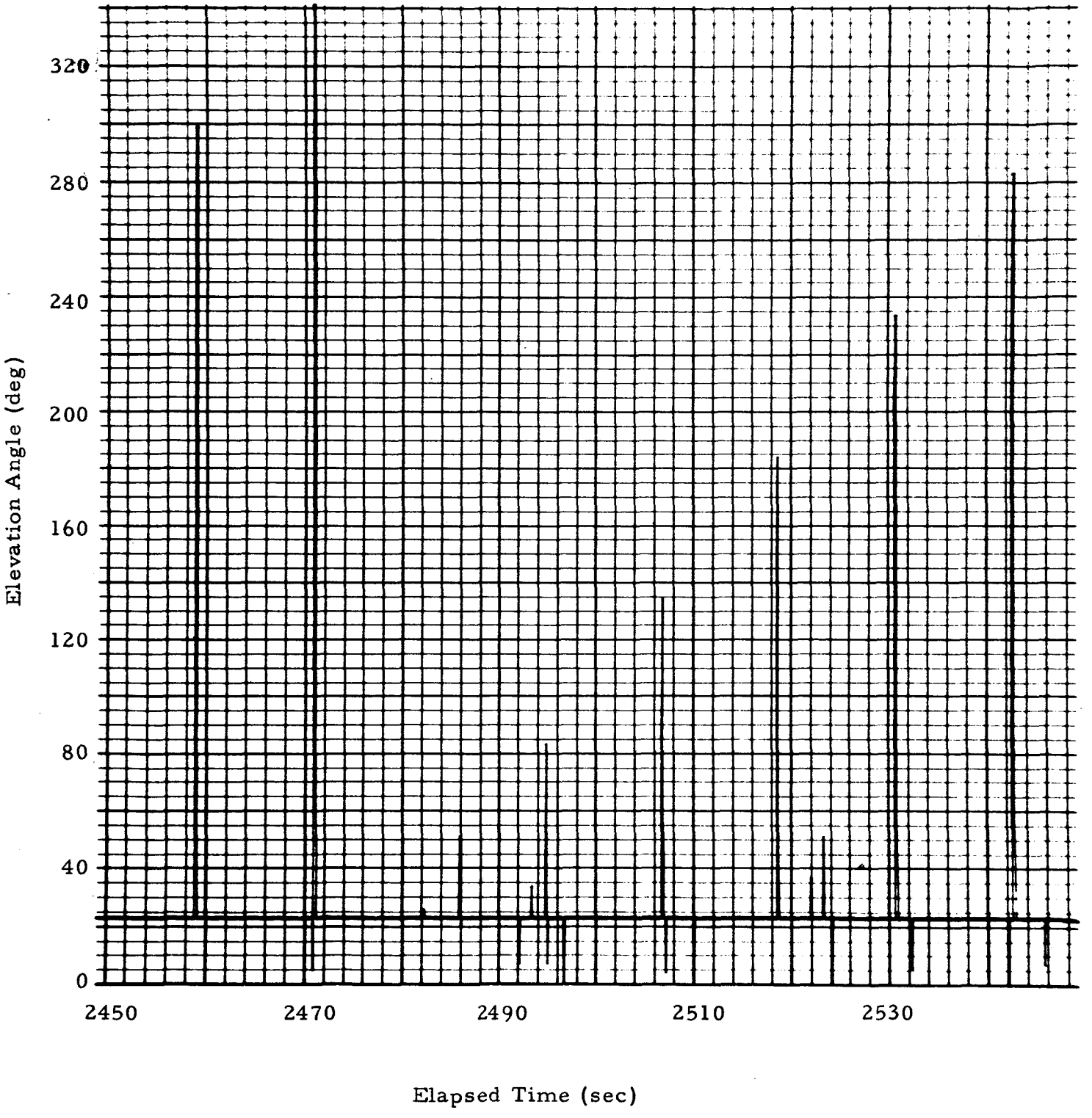

Fig. 5 - Periodic Occurrence of Stray Points

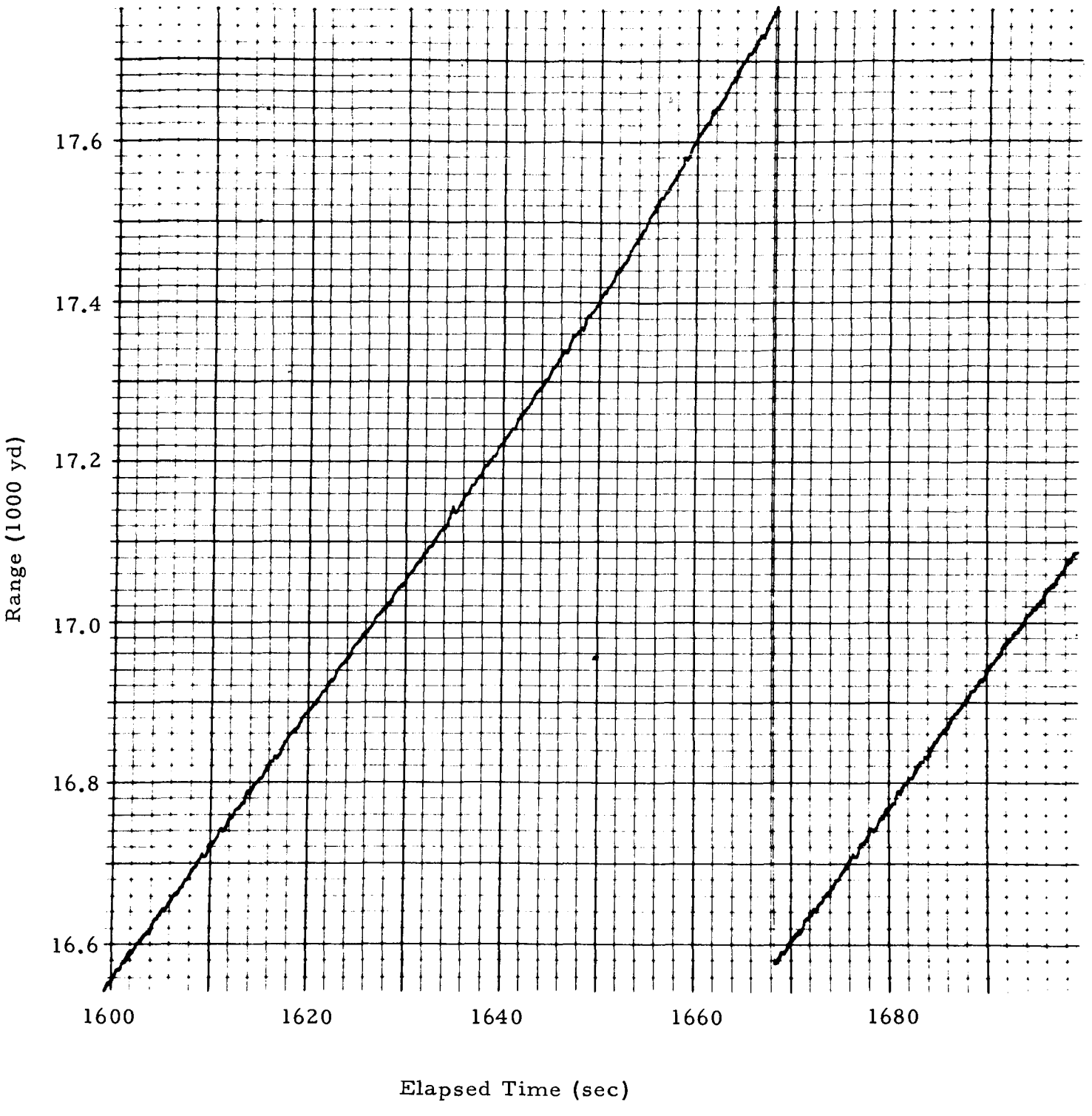

Fig. 6 - Overlapping (i.e. Repeating) Data Interval

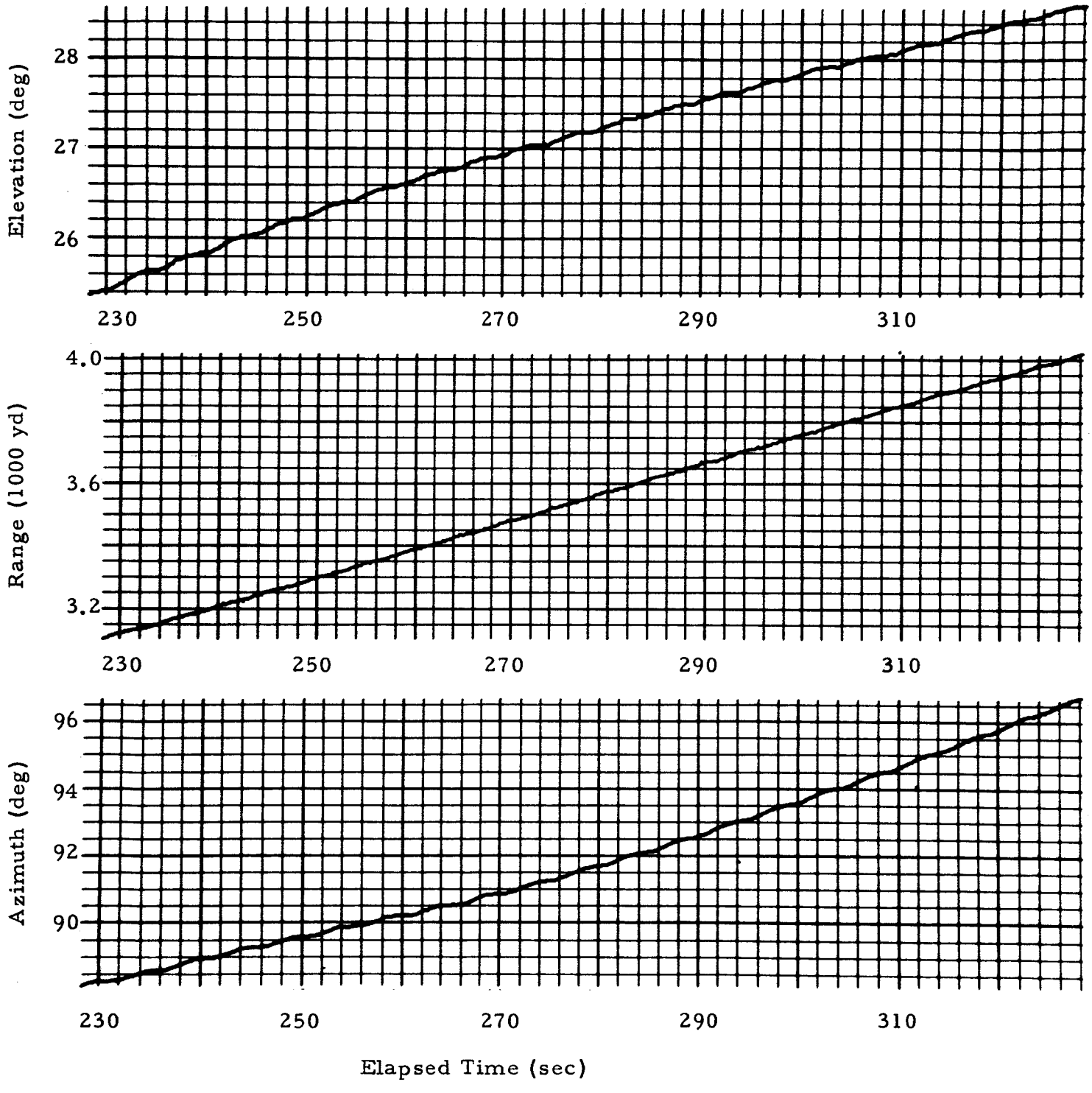

Fig. 7a - Example of 0.1-sec Data with Low Noise Level (TAER Measurements)

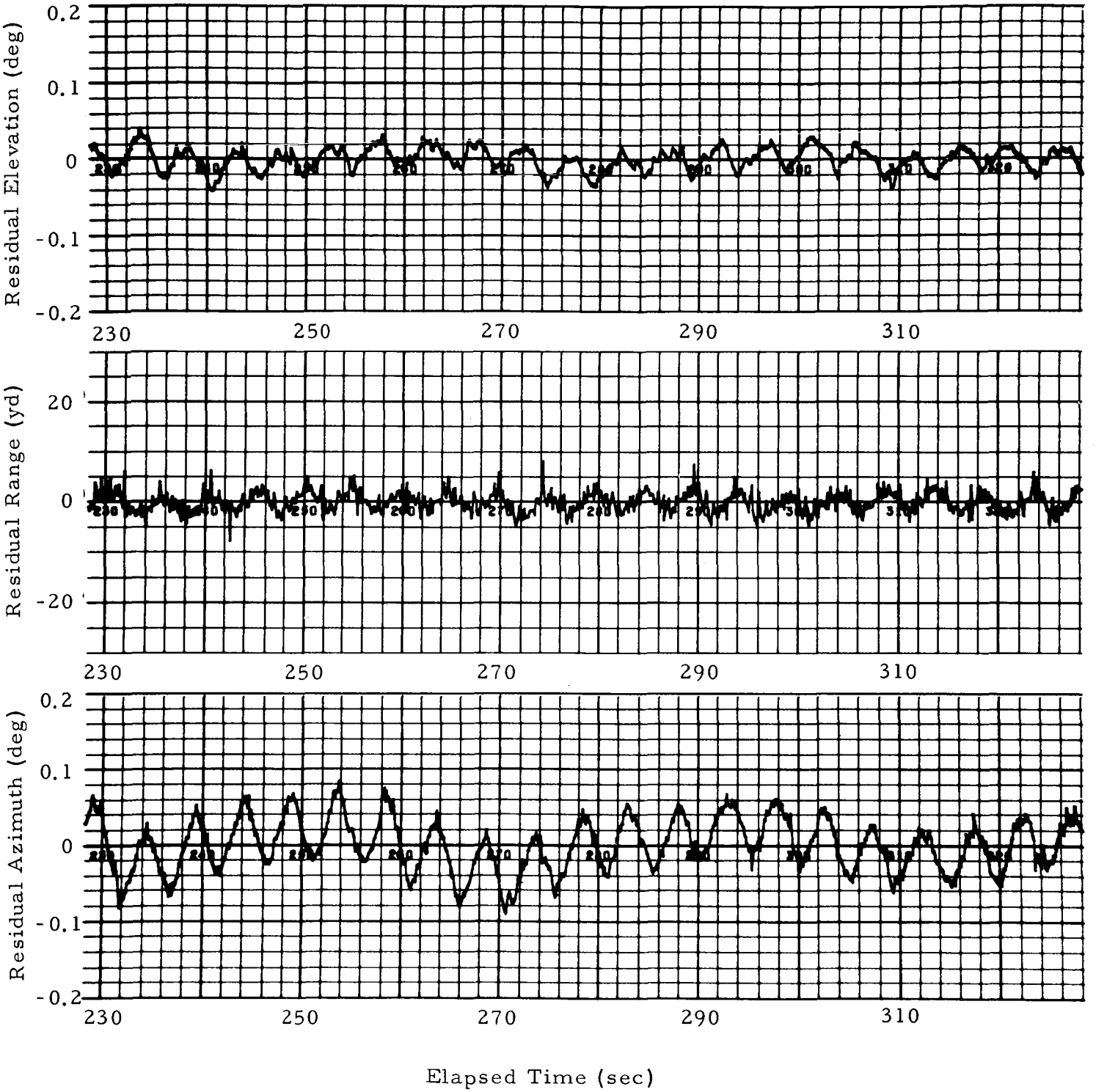

Fig. 7b - Example of 0.1-sec Data with Low Noise Level (Detrended TAER Measurements)

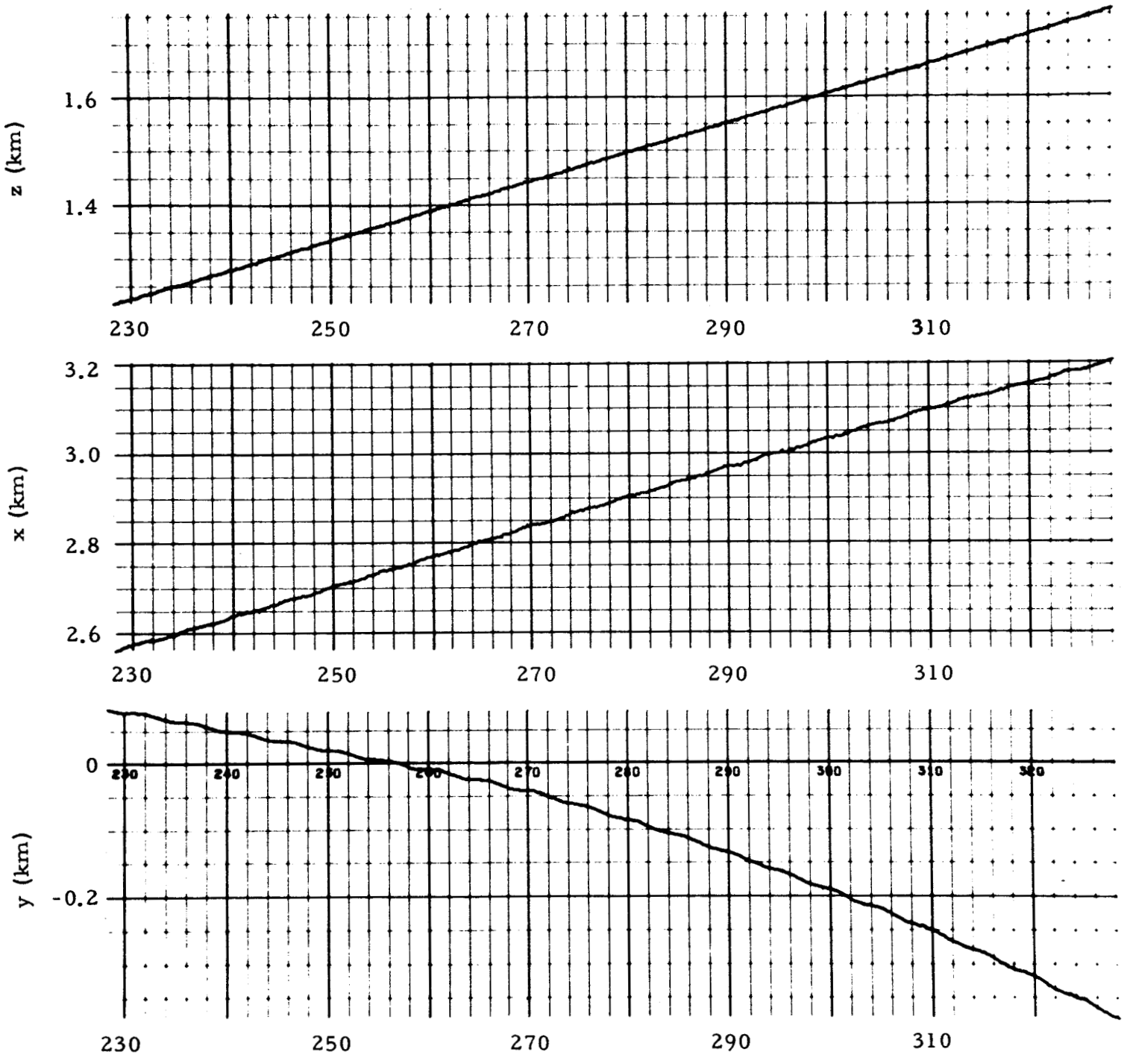

Fig. 7c - Example of 0.1-sec Data with Low Noise Level
(Computed xyz Position Coordinates)

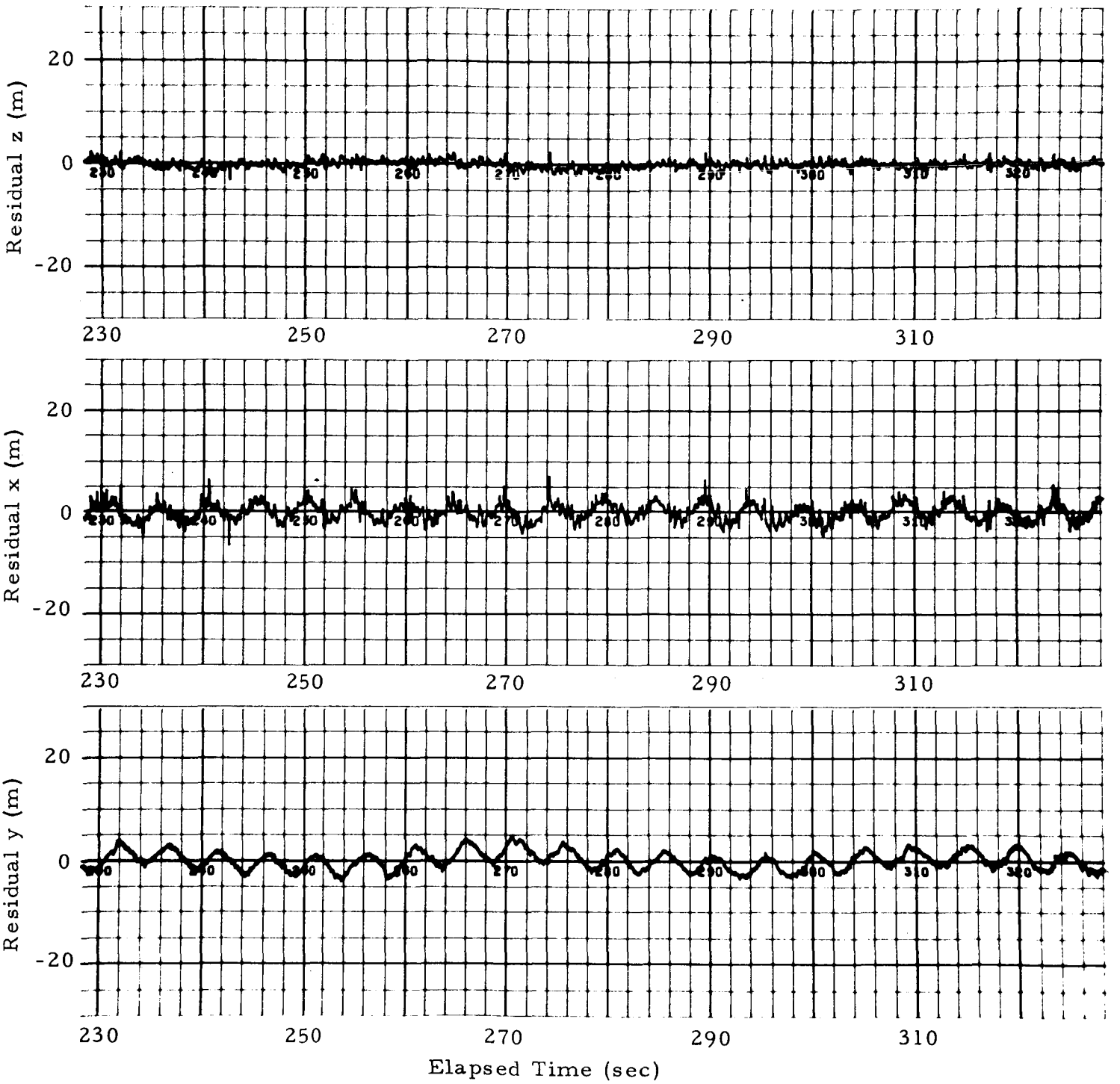

Fig. 7d - Example of 0.1-sec Data with Low Noise Level
(Detrended xyz Position Coordinates)

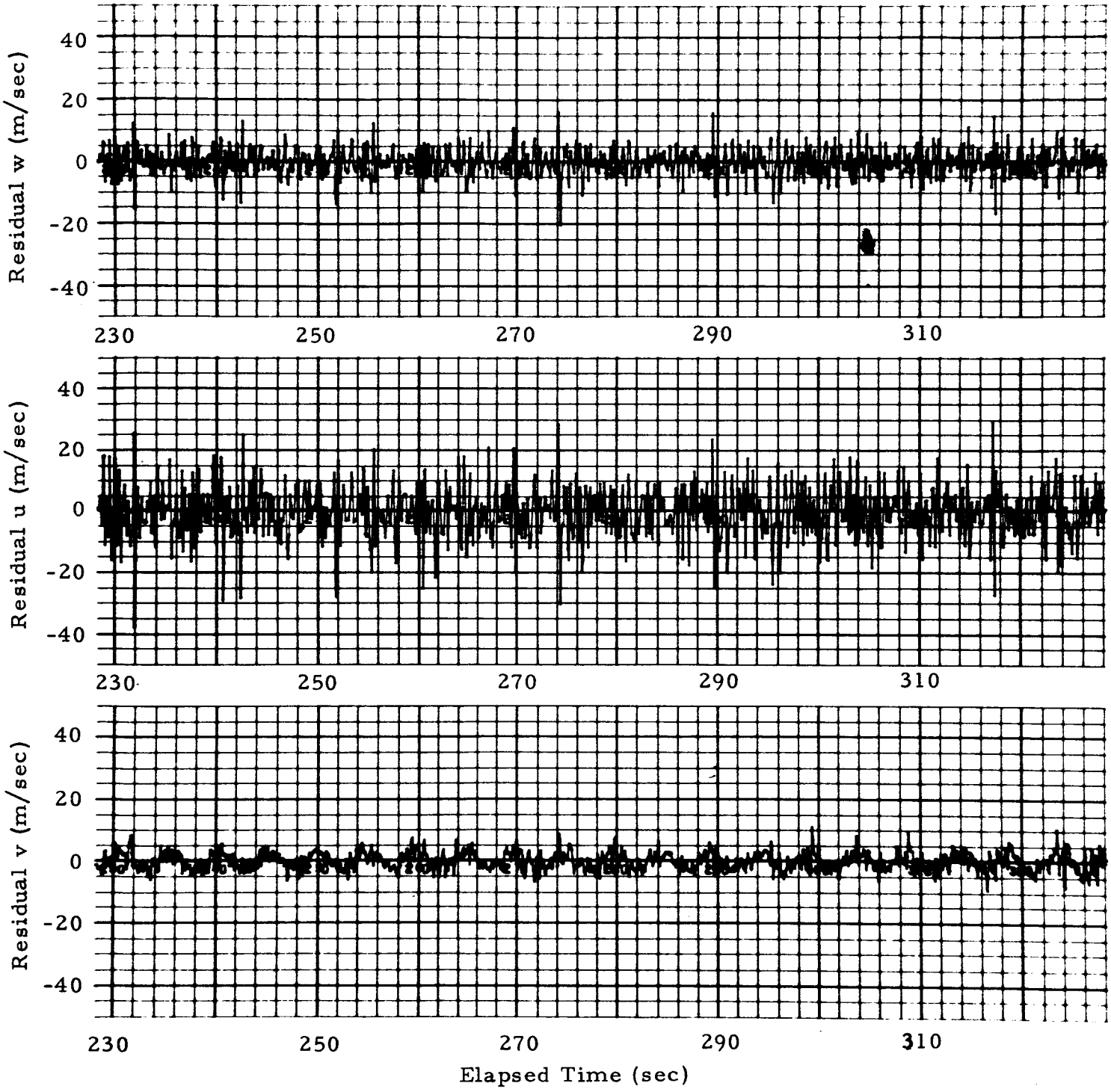

Fig. 7e - Example of 0.1-sec Data with Low Noise Level (Computed Velocity Residuals)

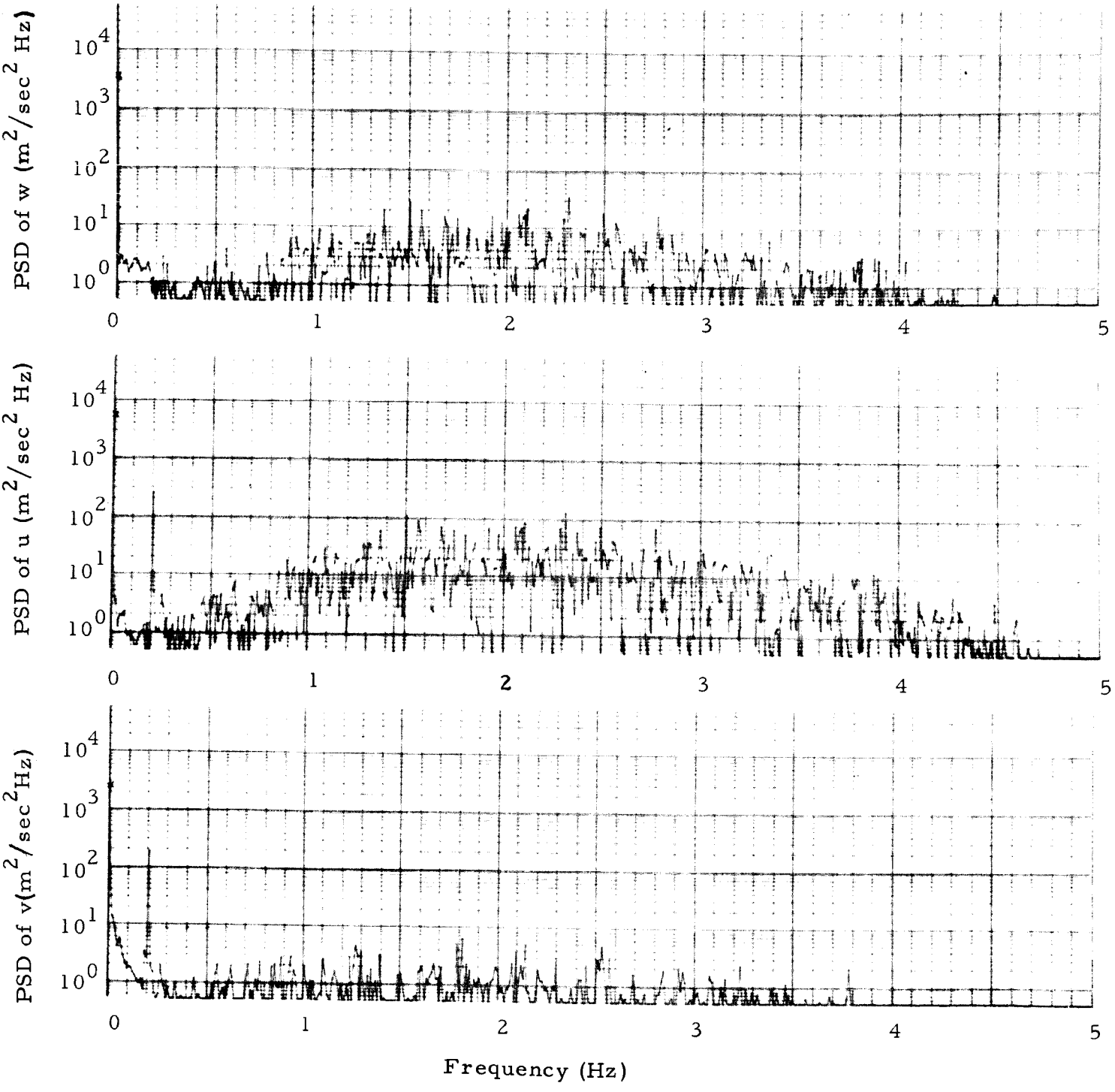

Fig. 7f - Example of 0.1-sec Data with Low Noise Level
(Power Spectral Density of Velocity Components)

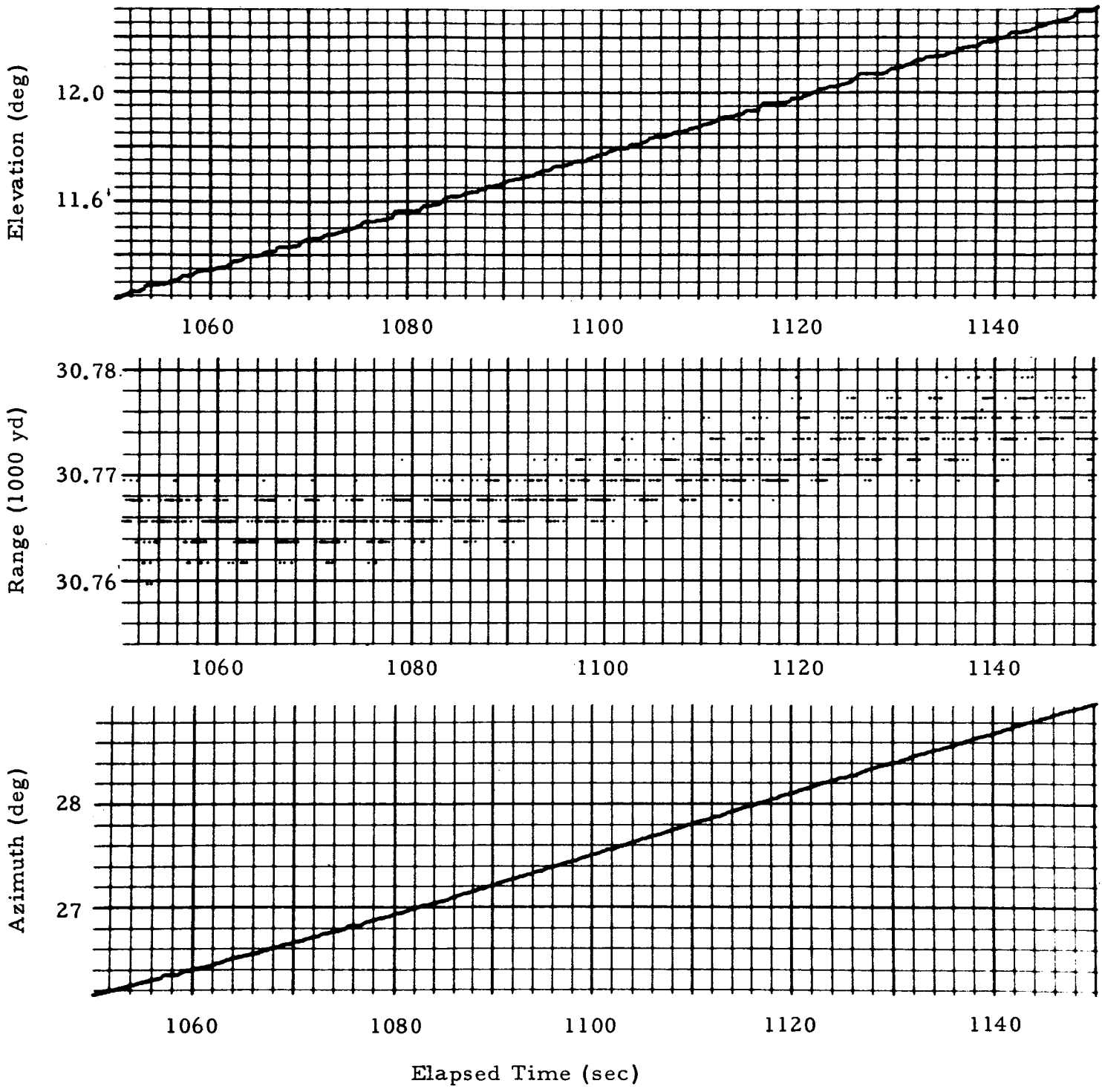

Fig. 8a - Example of 0.1-sec Data with Moderate Noise Level (TAER Measurements)

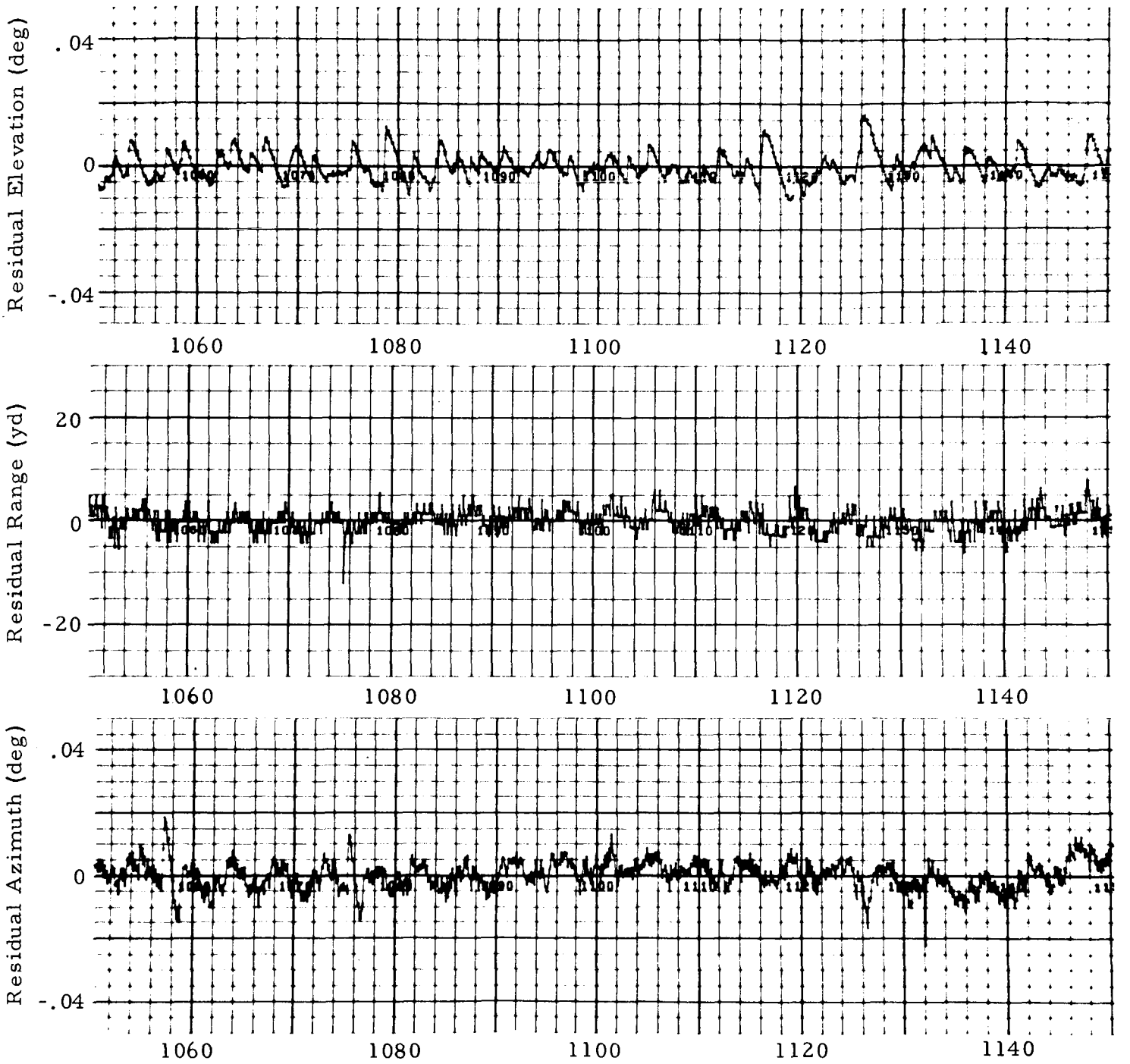

Fig. 8b - Example of 0.1-sec Data with Moderate Noise Level (Detrended TAER Measurements)

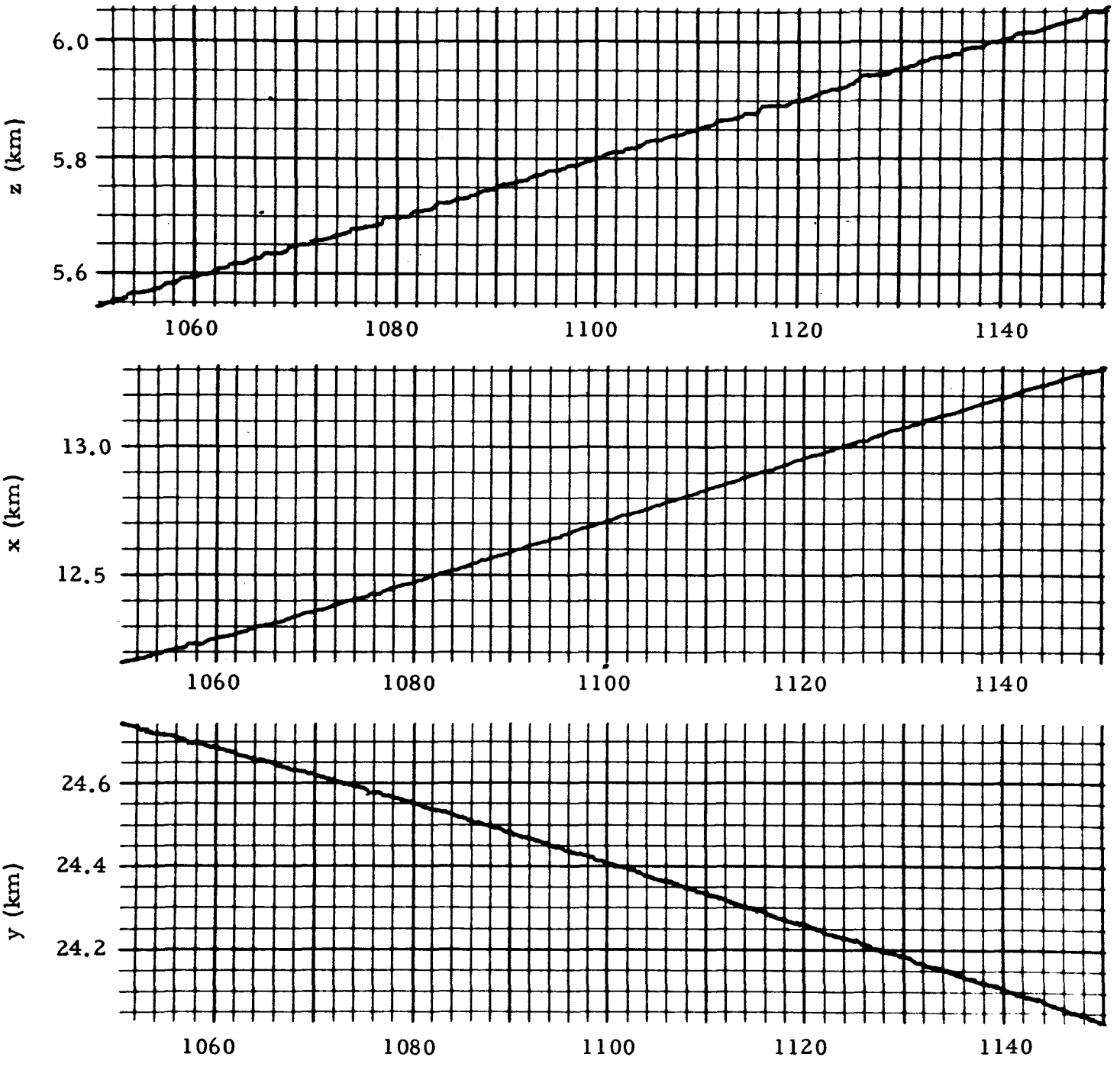

Fig. 8c - Example of 0.1-sec Data with Moderate Noise Level
(Computed xyz Position Coordinates)

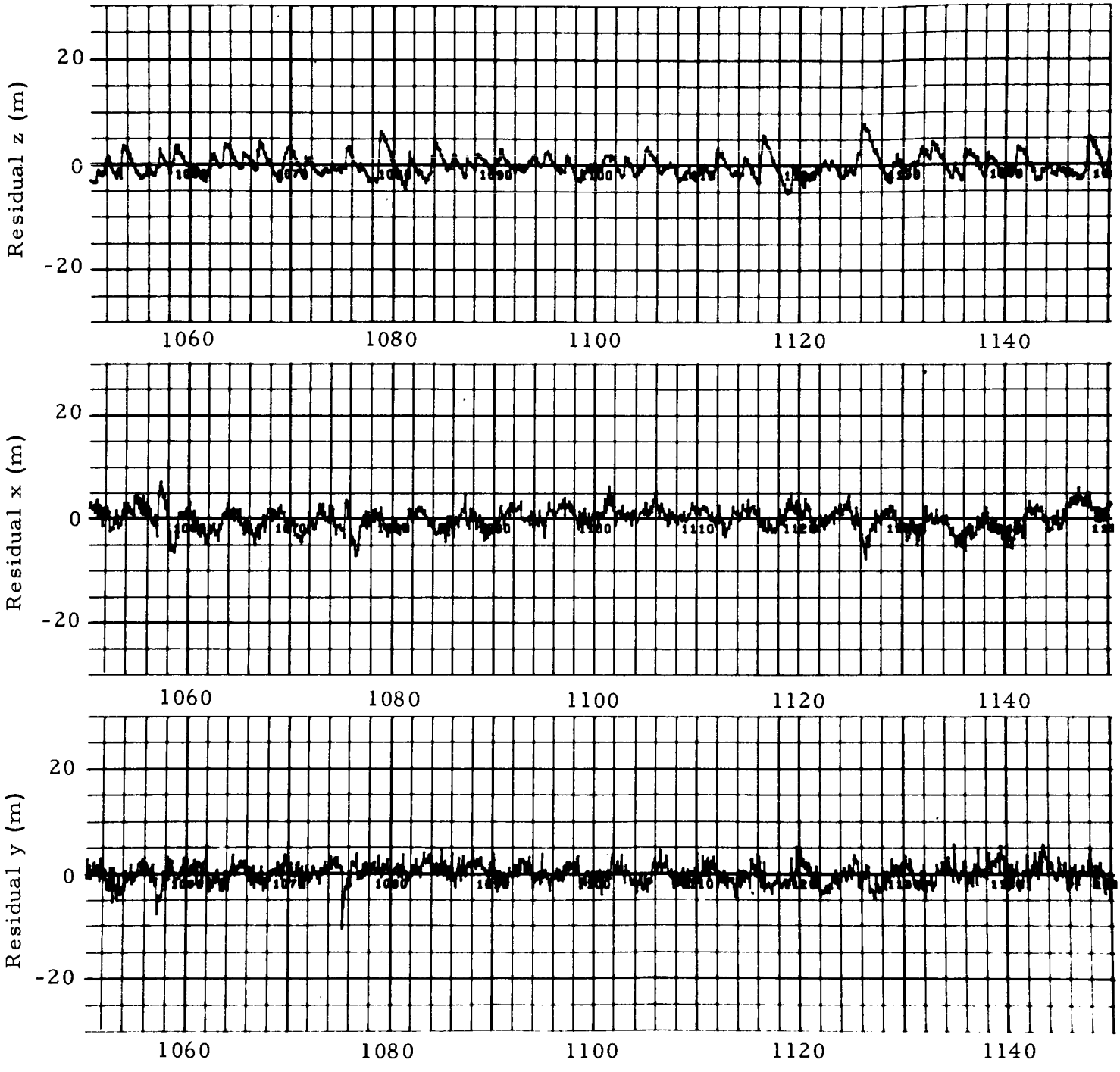

Fig. 8d - Example of 0.1-sec Data with Moderate Noise Level
(Detrended xyz Position Coordinates)

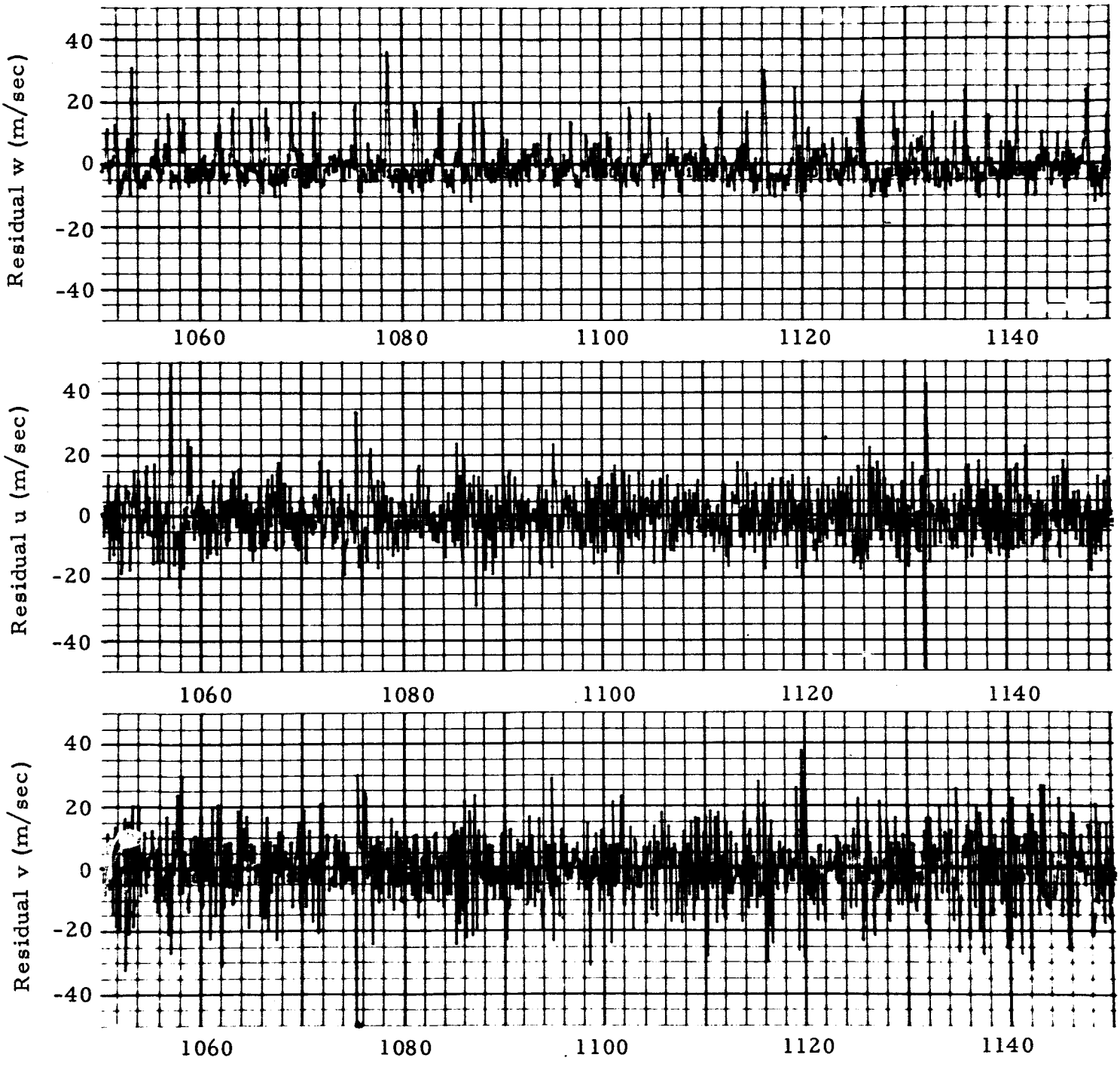

Fig. 8e - Example of 0.1-sec Data with Moderate Noise Level (Computed Velocity Residuals)

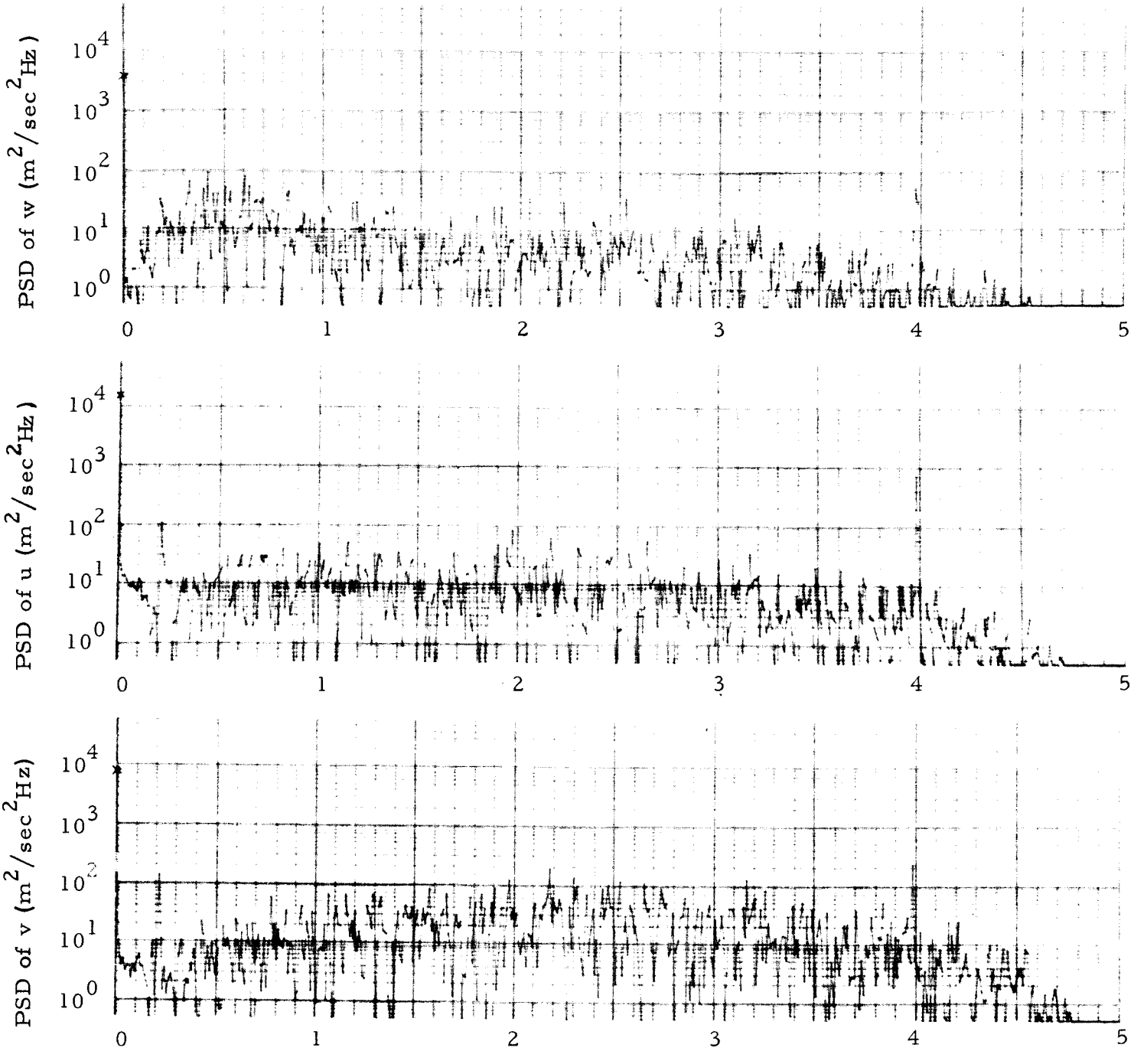

Fig. 8f - Example of 0.1-sec Data with Moderate Noise Level (Power Spectral Density of Velocity Components)

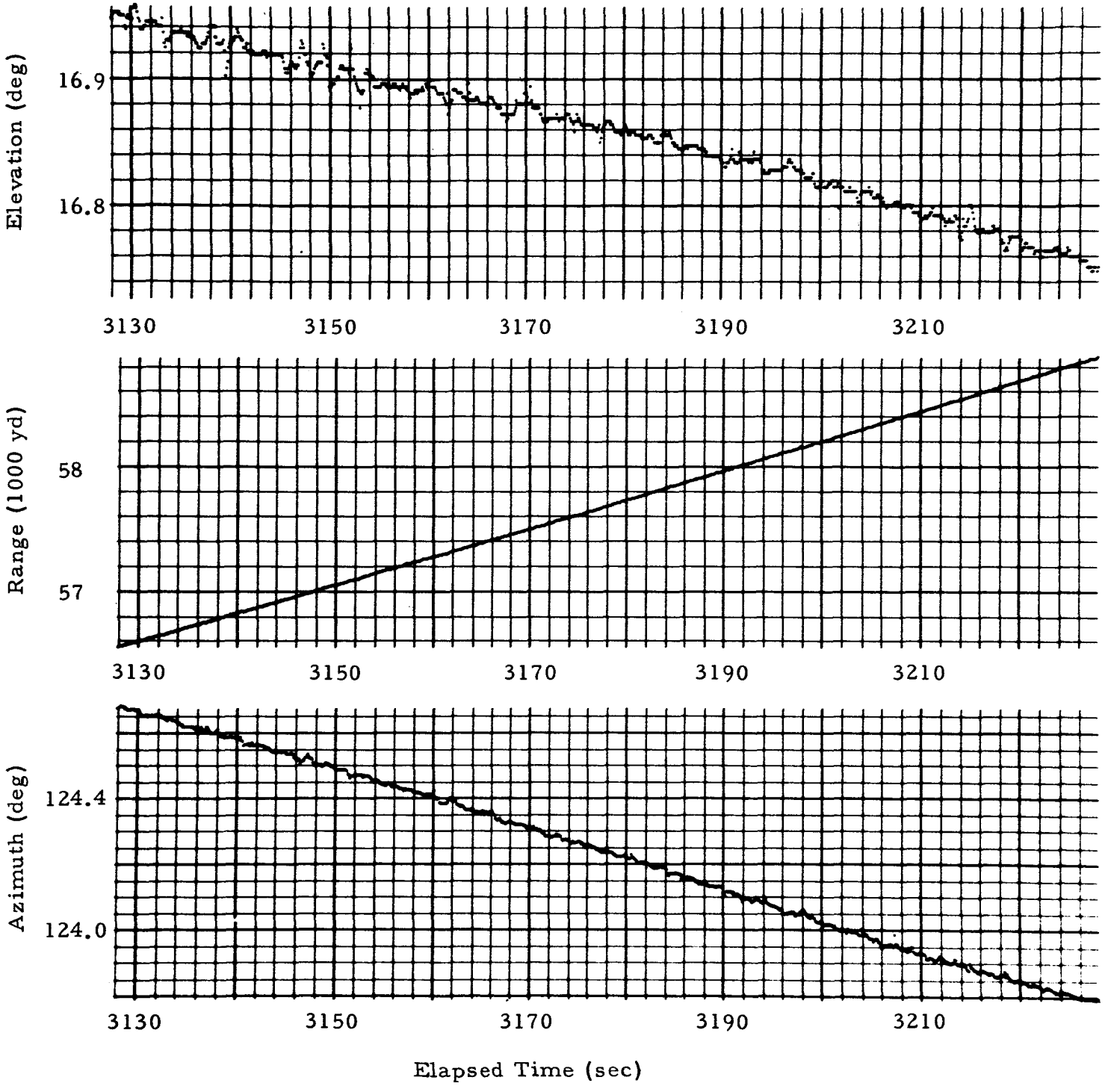

Fig. 9a - Example of 0.1-sec Data with High Noise Level (TAER Measurements)

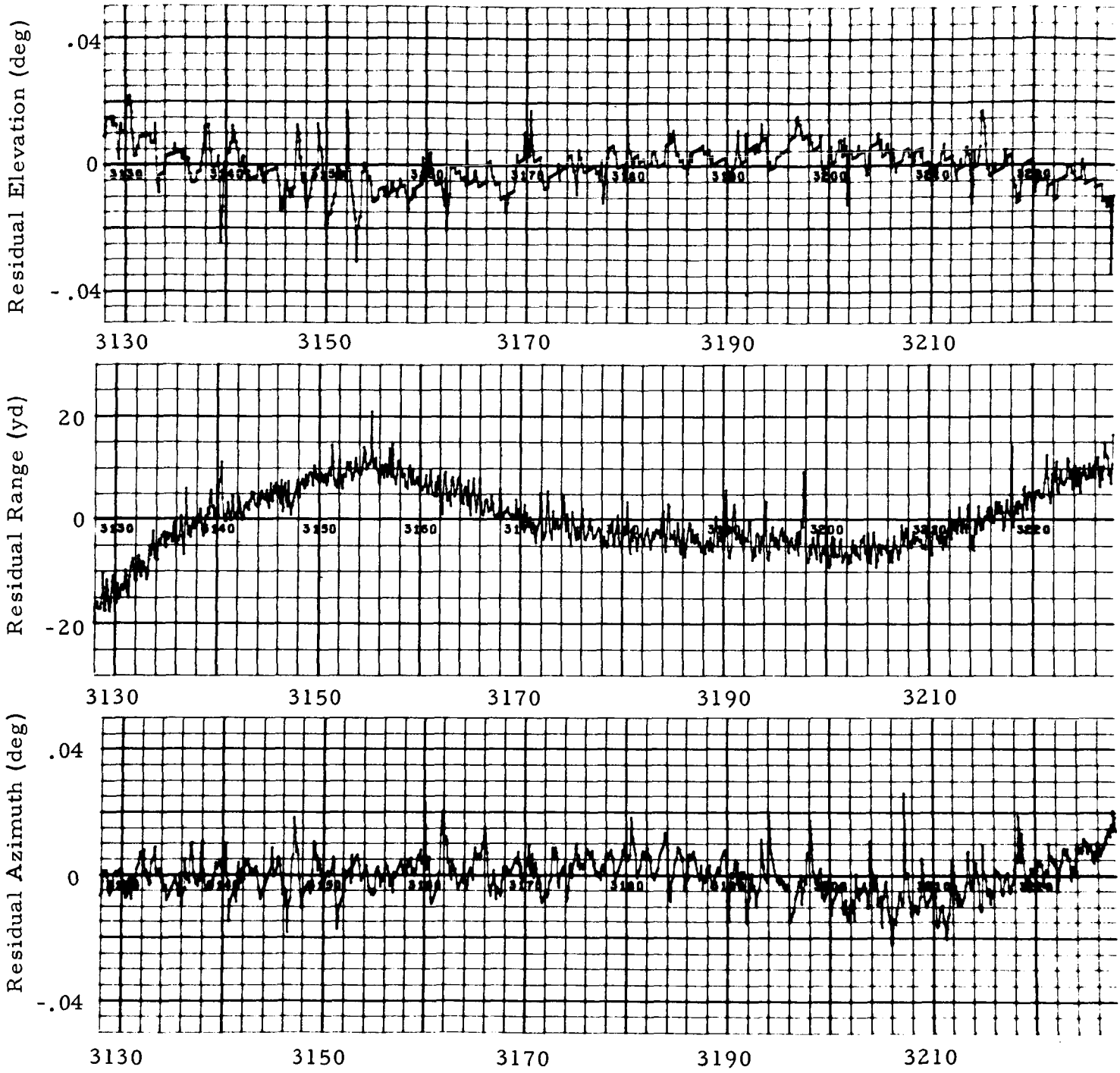

Fig. 9b - Example of 0.1-sec Data with High Noise Level
(Detrended TAER Measurements)

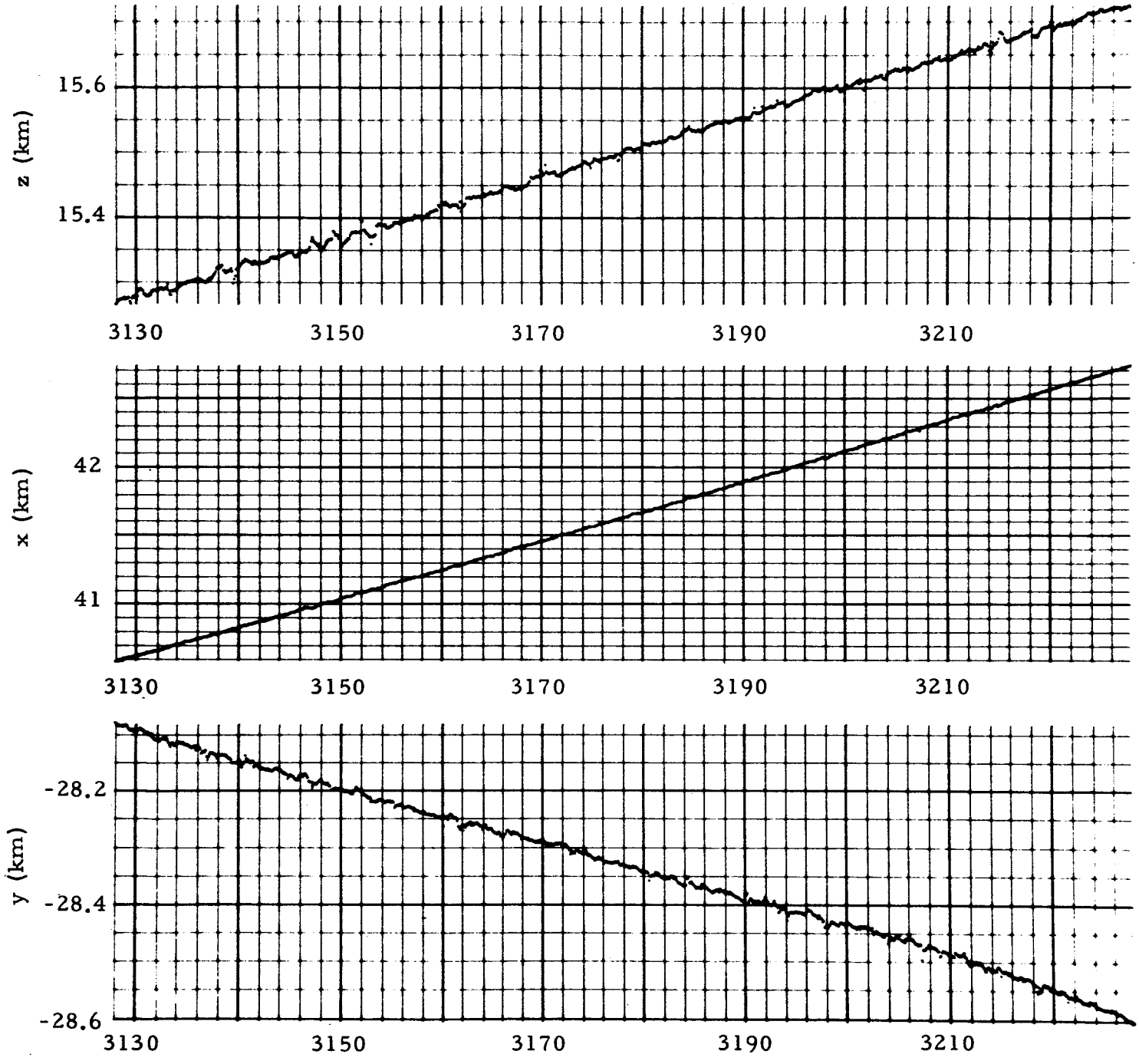

Fig. 9c - Example of 0.1-sec Data with High Noise Level
(Computed xyz Position Coordinates)

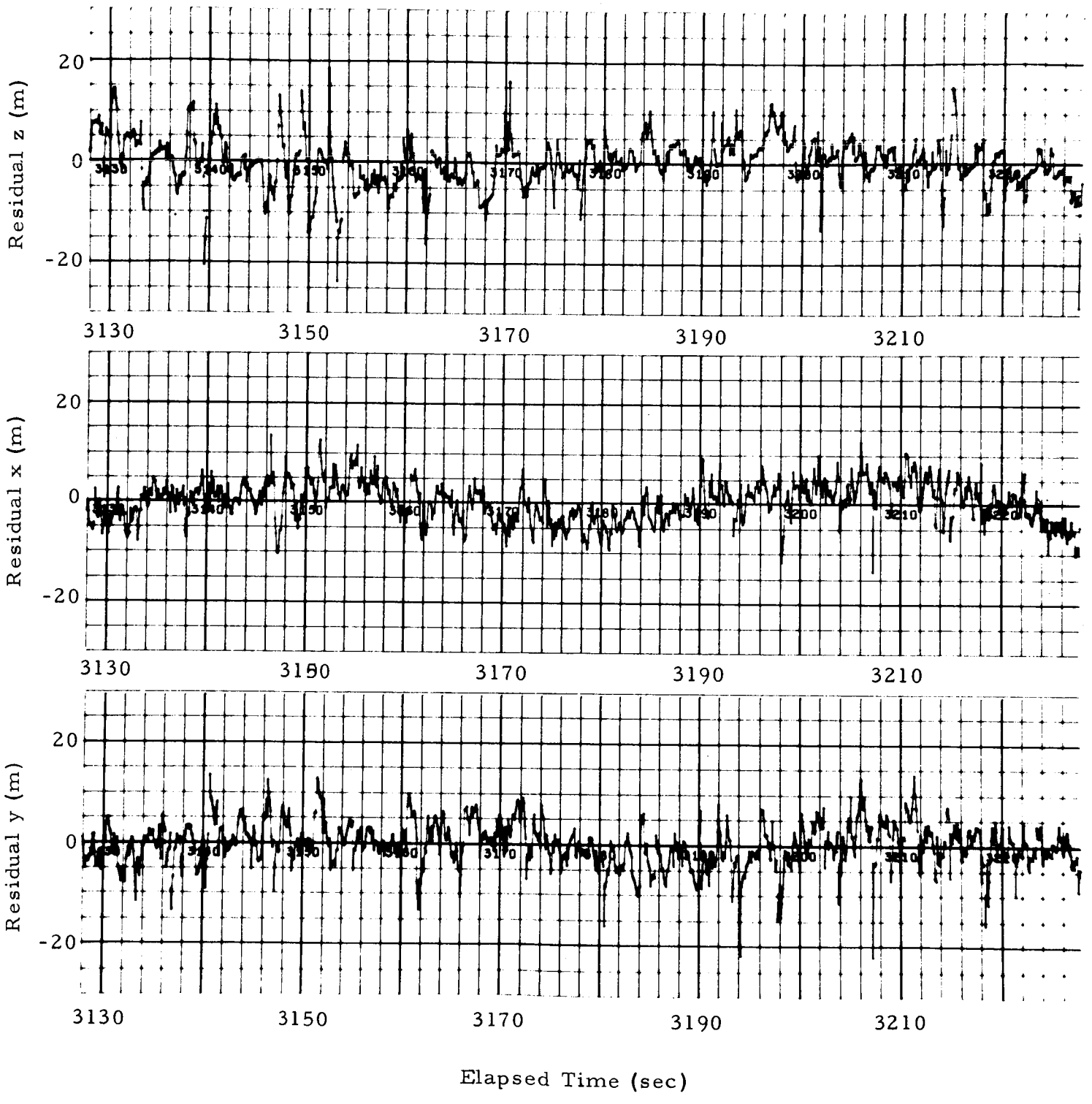

Fig. 9d - Example of 0.1-sec Data with High Noise Level
(Detrended xyz Position Coordinates)

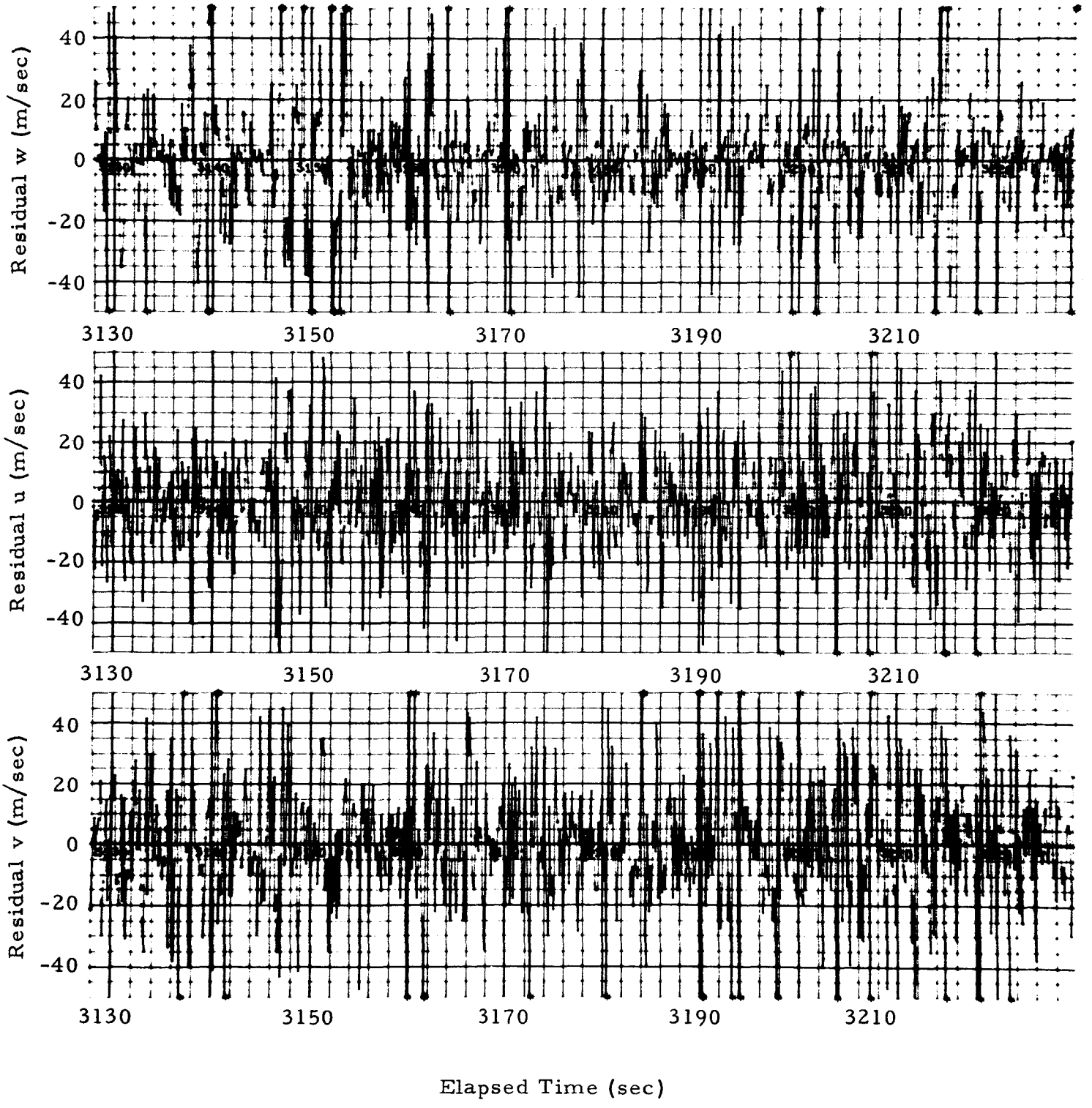

Fig. 9e - Example of 0.1-sec Data with High Noise Level
(Computed Velocity Residuals)

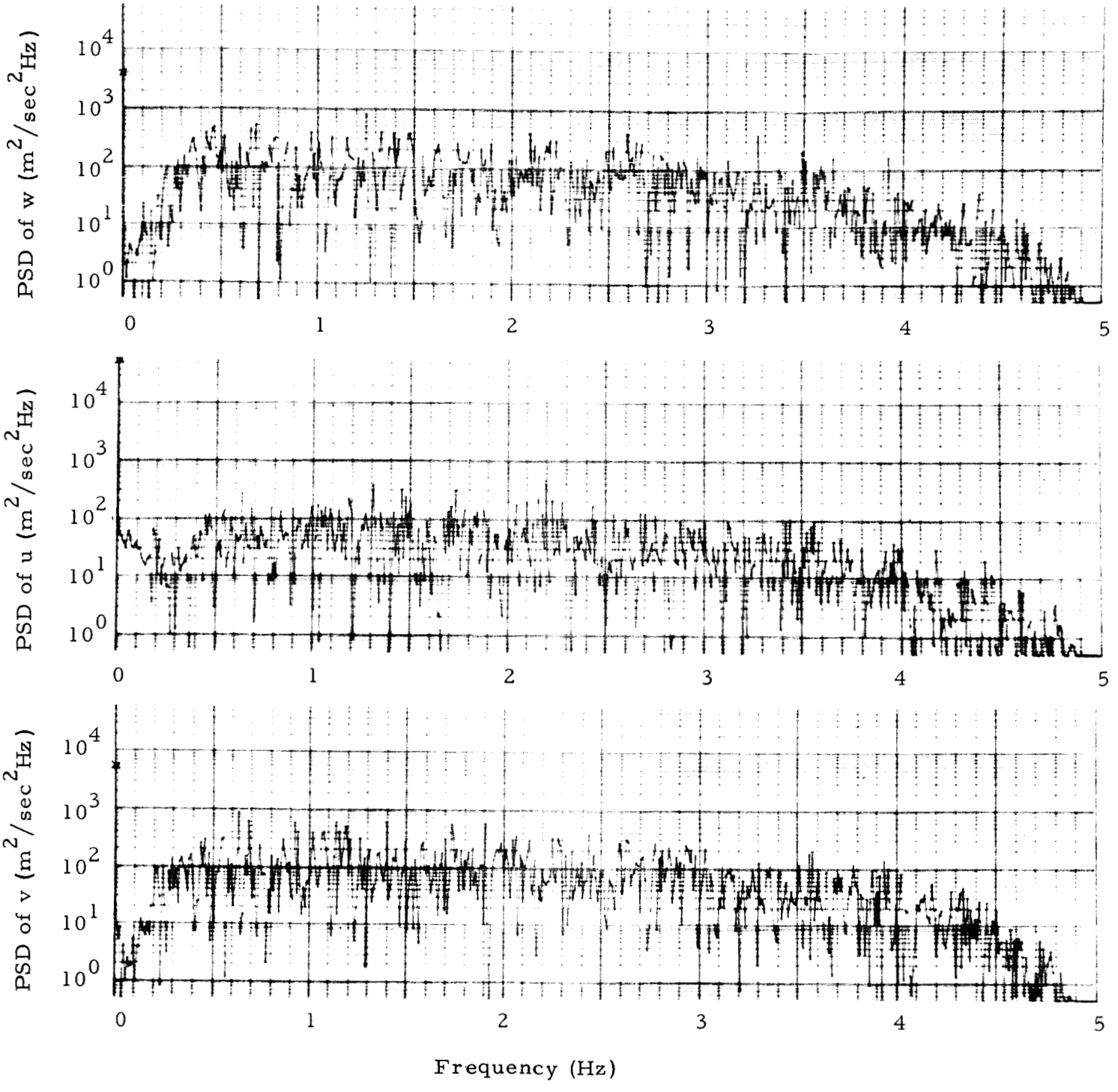

Fig. 9f - Example of 0.1-sec Data with High Noise Level
(Power Spectral Density of Velocity Components)

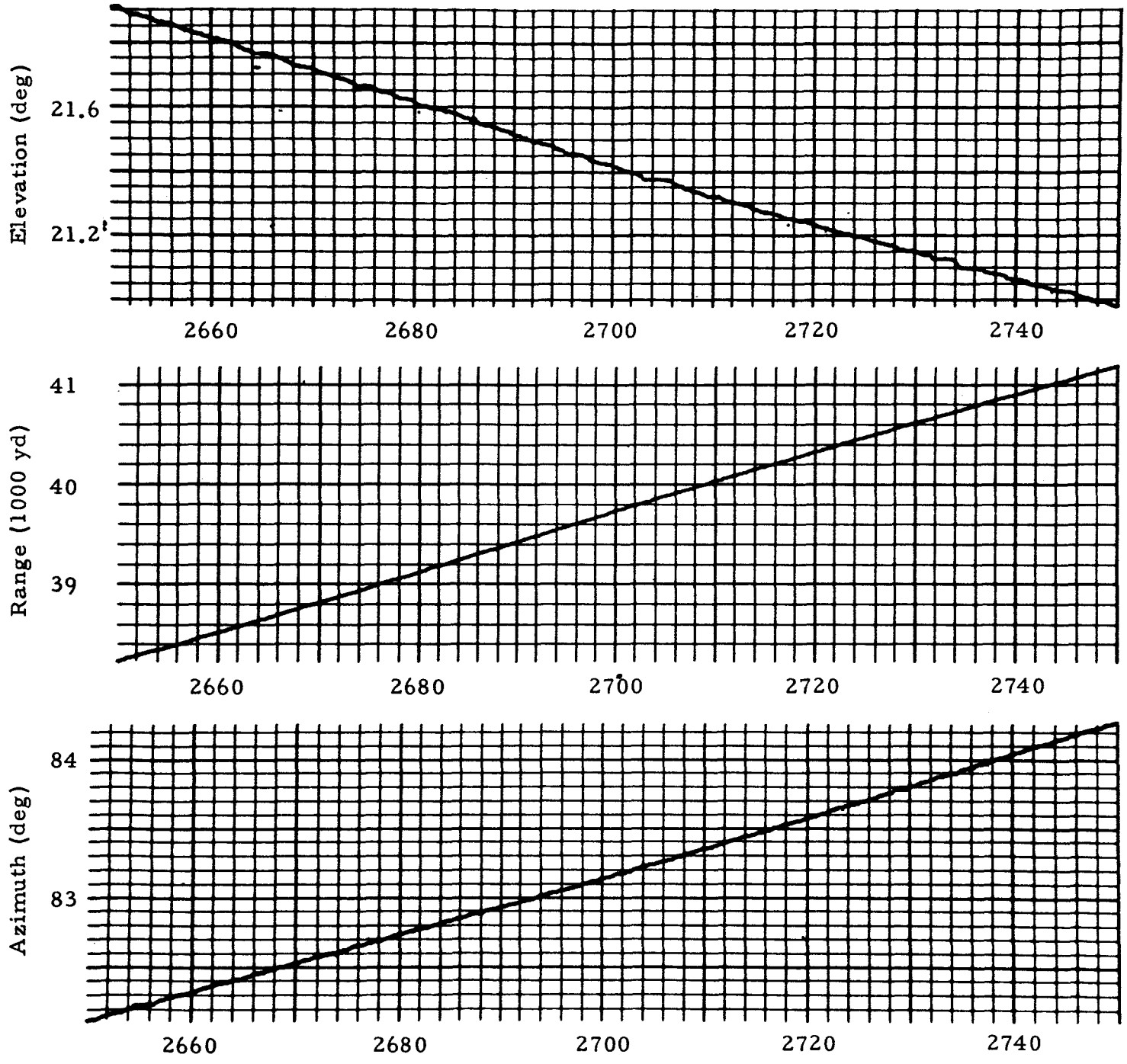

Fig. 10a - Example of Stray Points in Edited 0.1-sec Data (TAER Measurements)

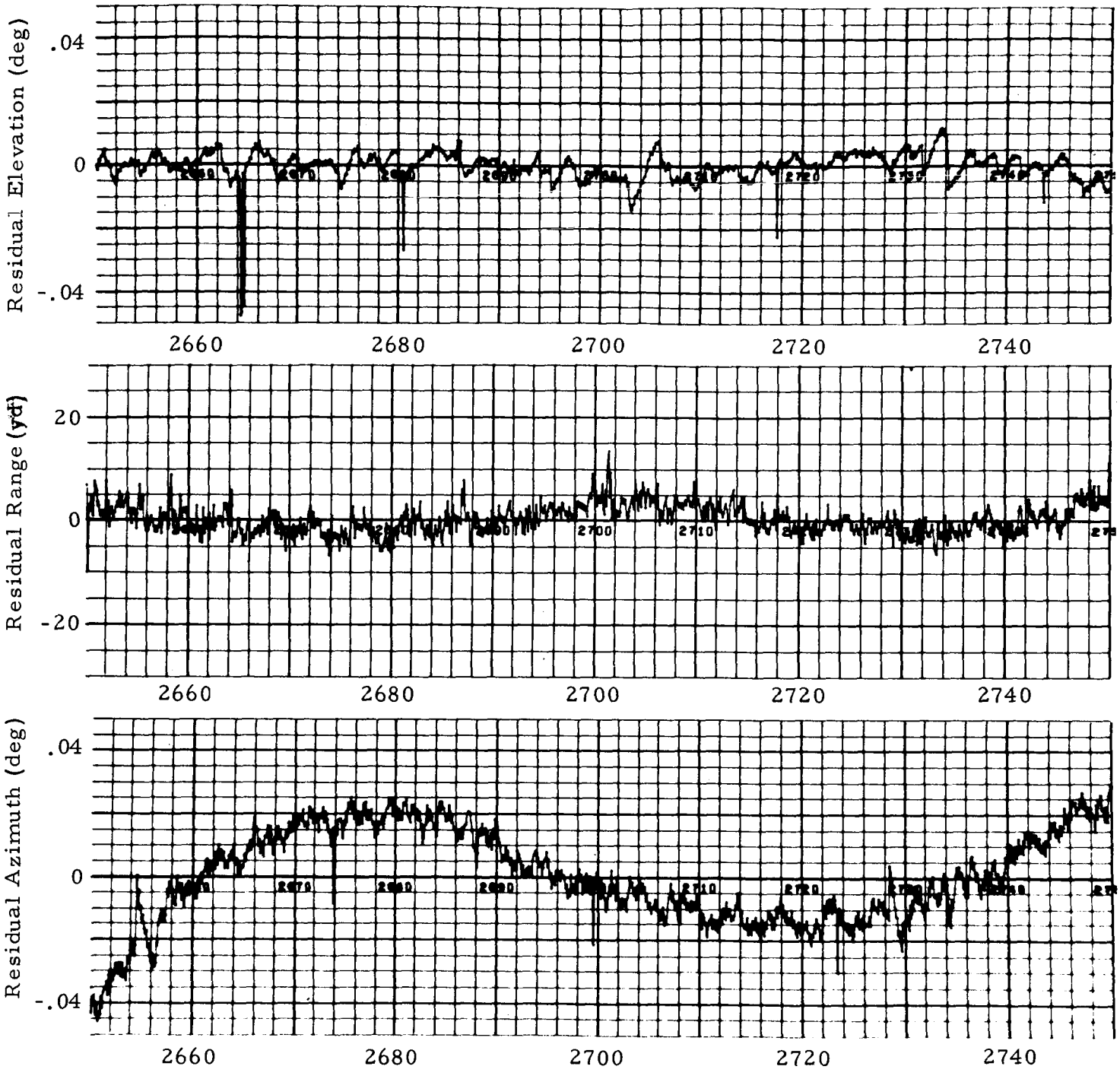

Fig. 10b - Example of Stray Points in Edited 0.1-sec Data (Detrended TAER Measurements)

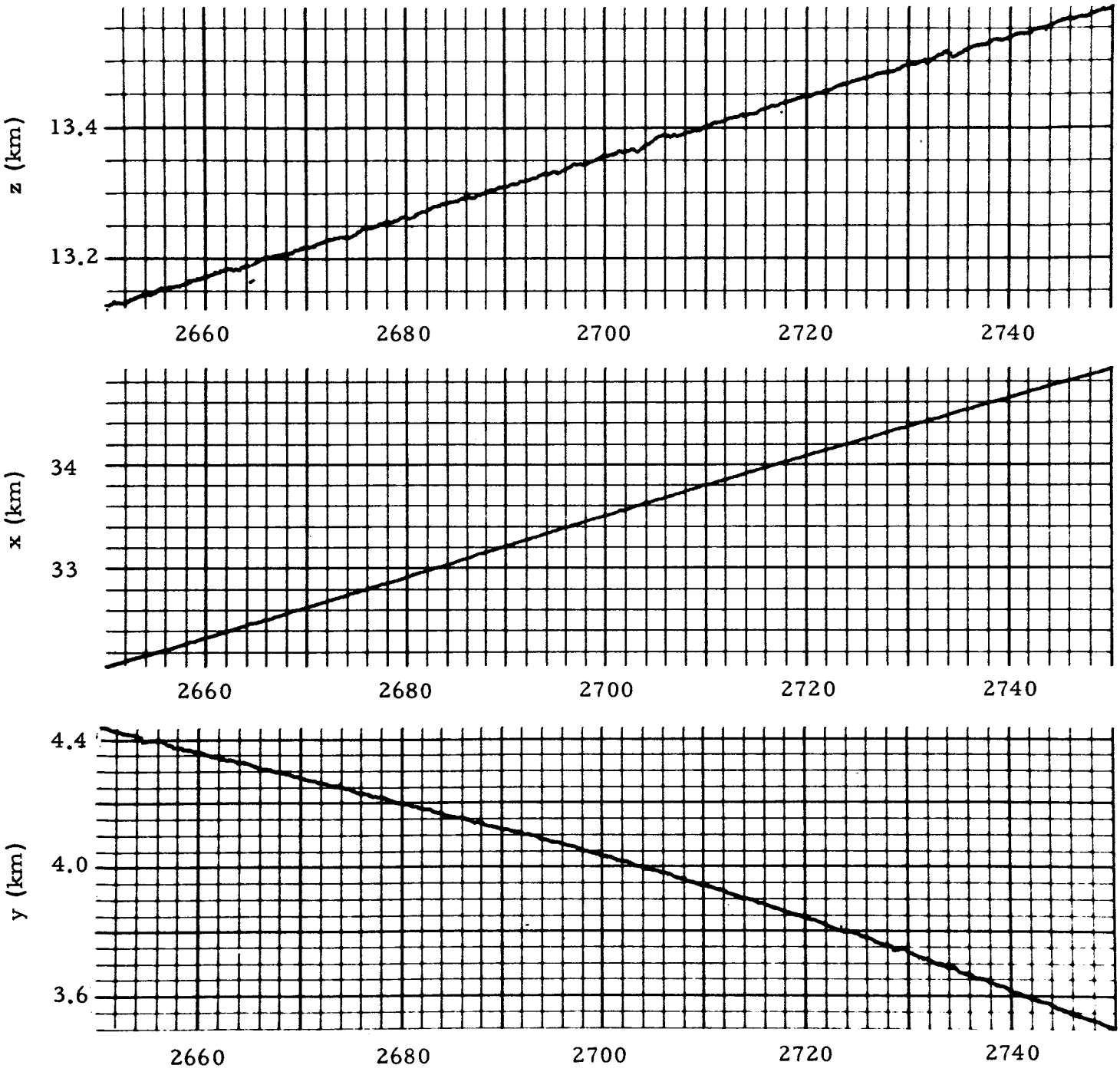

Fig. 10c - Example of Stray Points in Edited 0.1-sec Data (Computed xyz Position Coordinates)

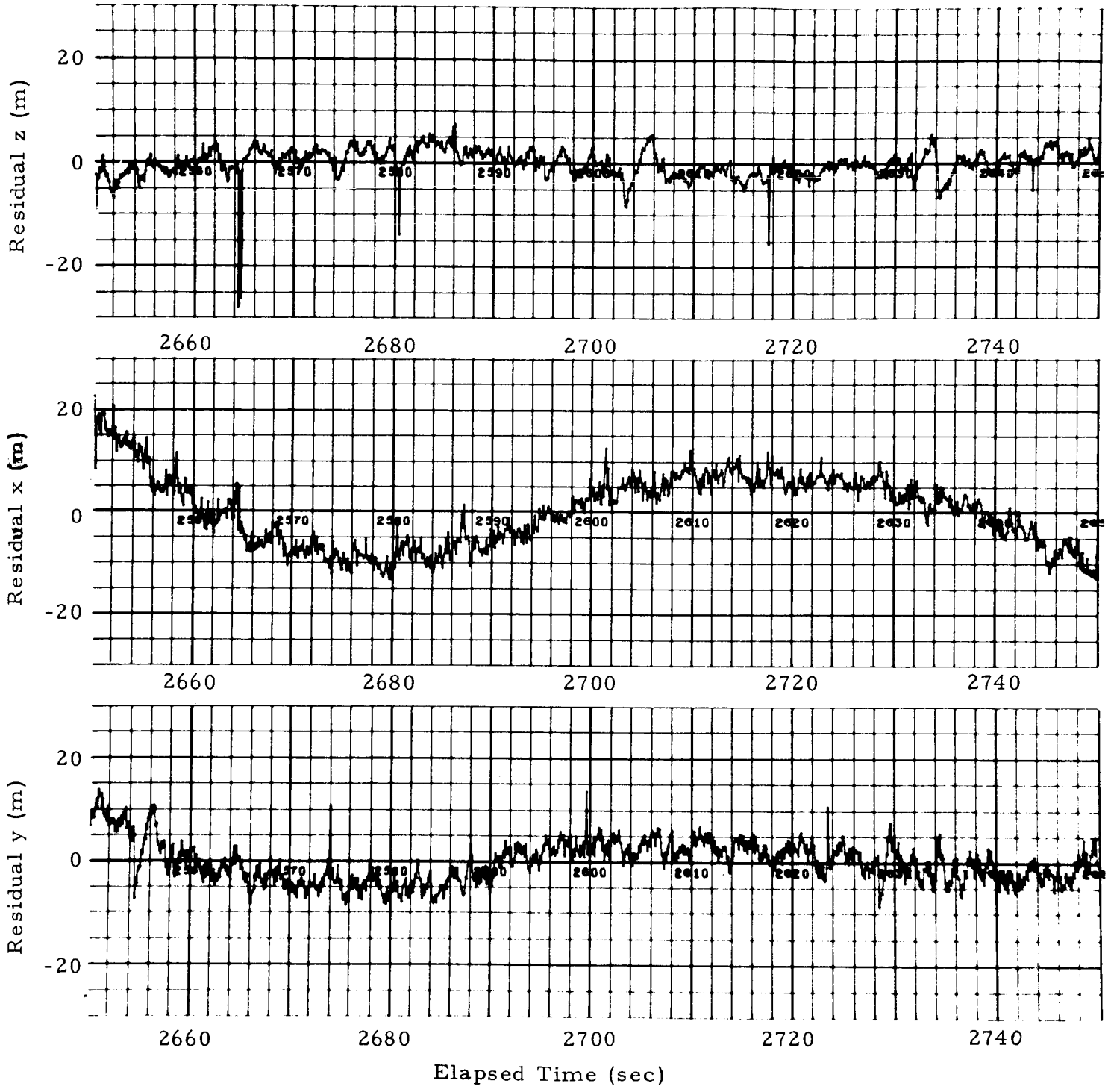

Fig. 10d - Example of Stray Points in Edited 0.1-sec Data
(Detrended xyz Position Coordinates)

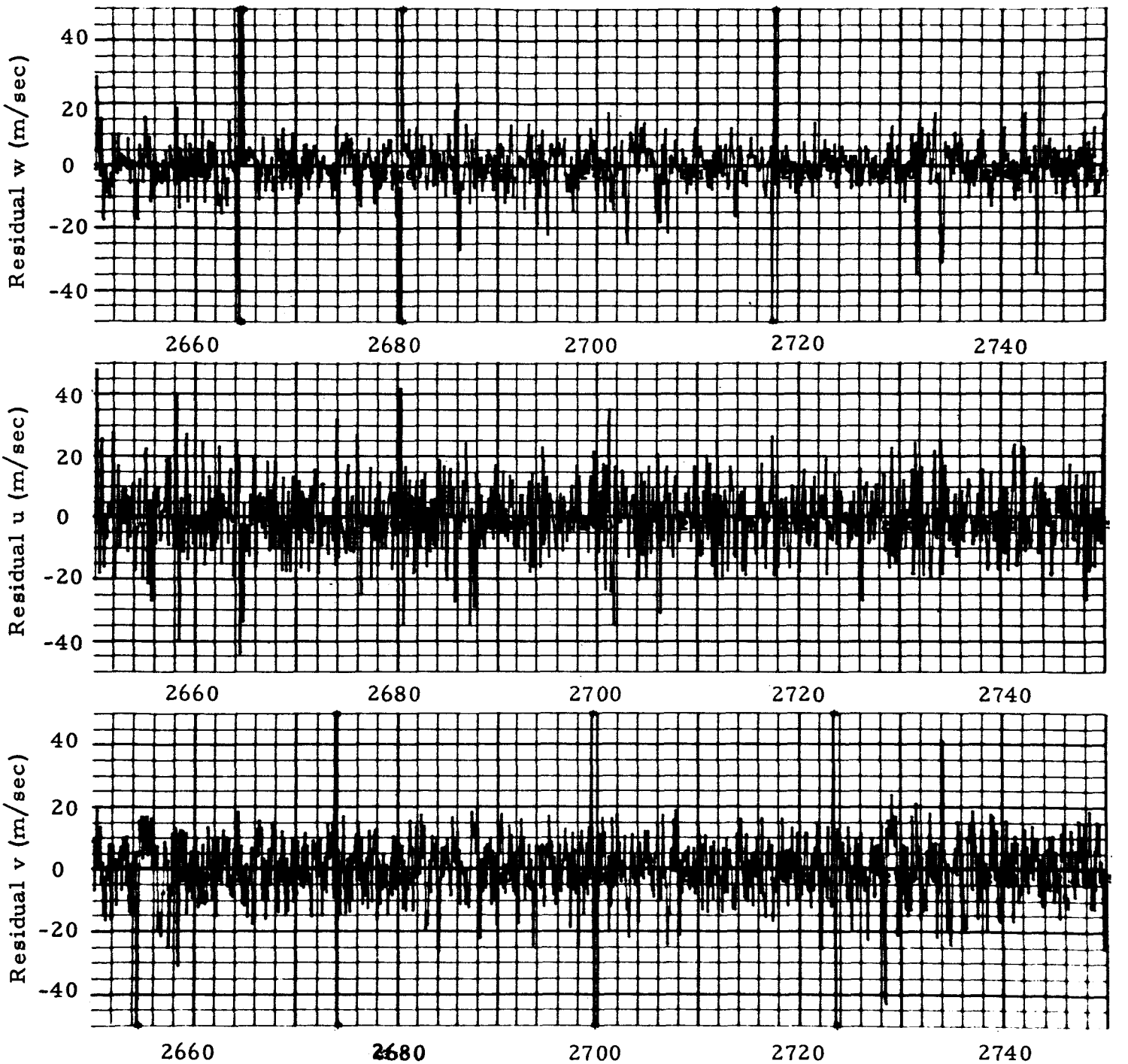

Fig. 10e - Example of Stray Points in Edited 0.1-sec Data
(Computed Velocity Residuals)

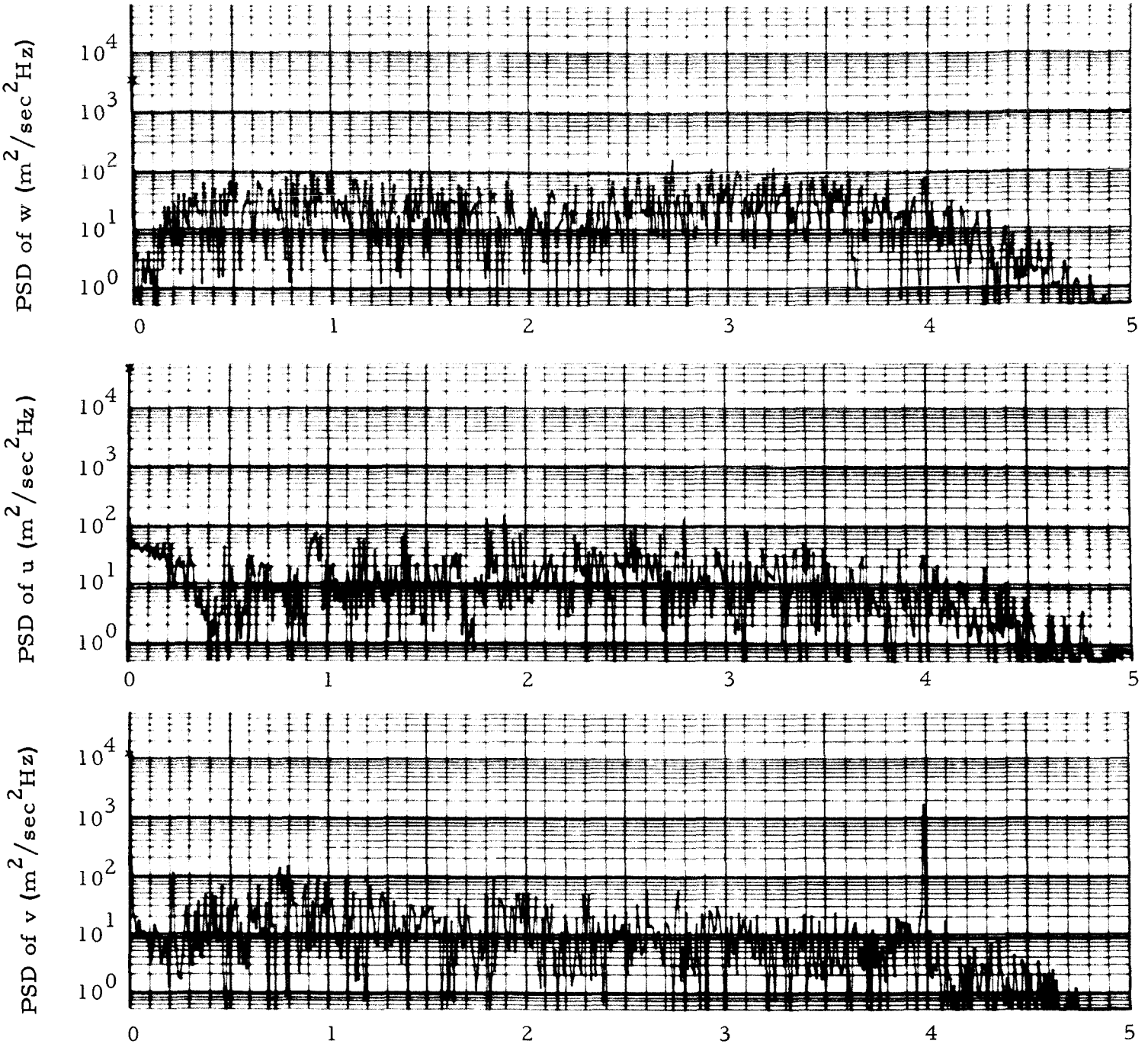

Fig. 10f - Example of Stray Points in Edited 0.1-sec Data
(Power Spectral Density of Velocity Components)

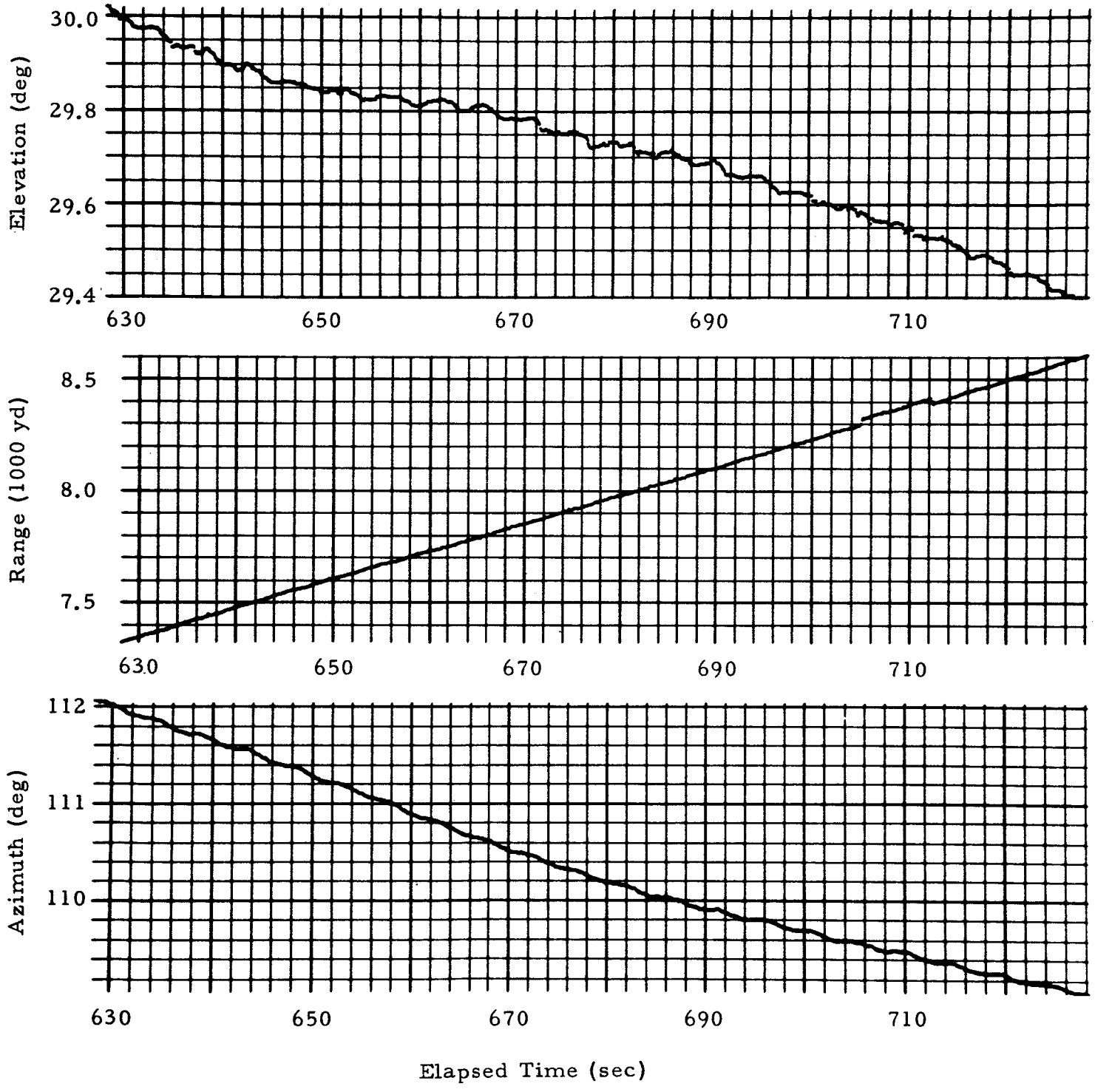

Fig. 11a - Example of Data Shift in Edited 0.1-sec Data (TAER Measurements)

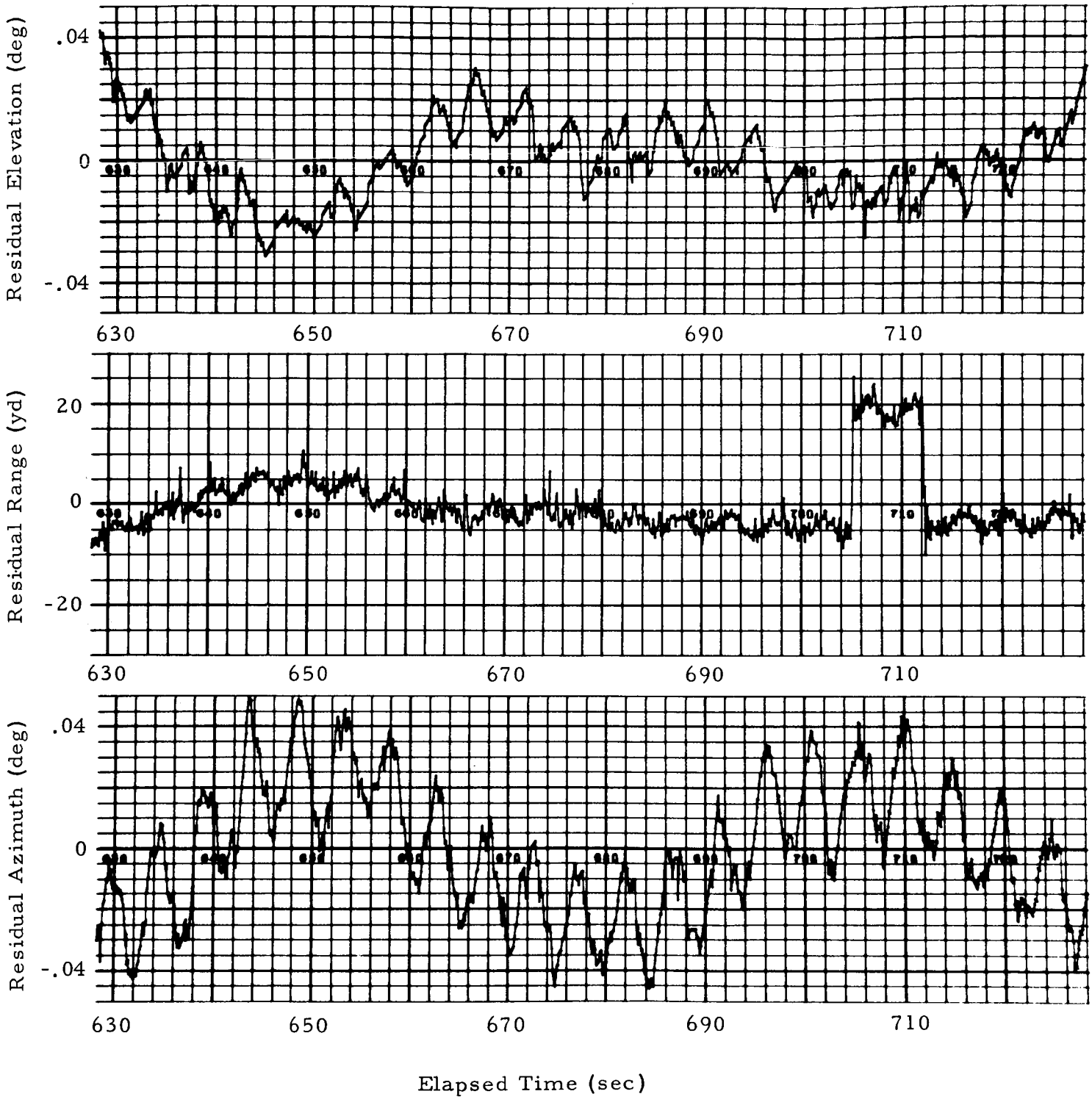

Fig. 11b - Example of Data Shift in Edited 0.1-sec Data
(Detrended TAER Measurements)

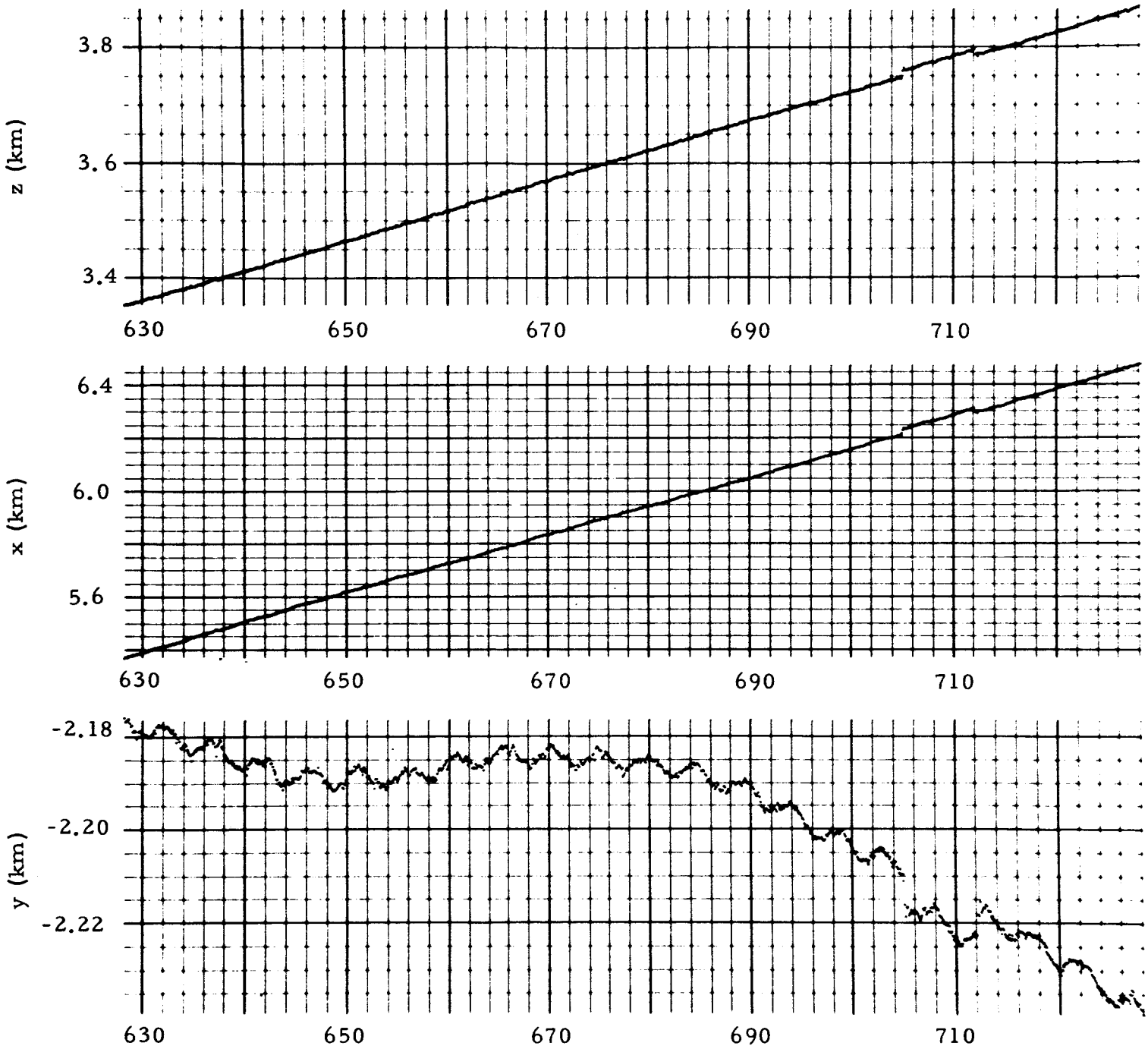

Fig. 11c - Example of Data Shift in Edited 0.1-sec Data
(Computed x y z Position Coordinates)

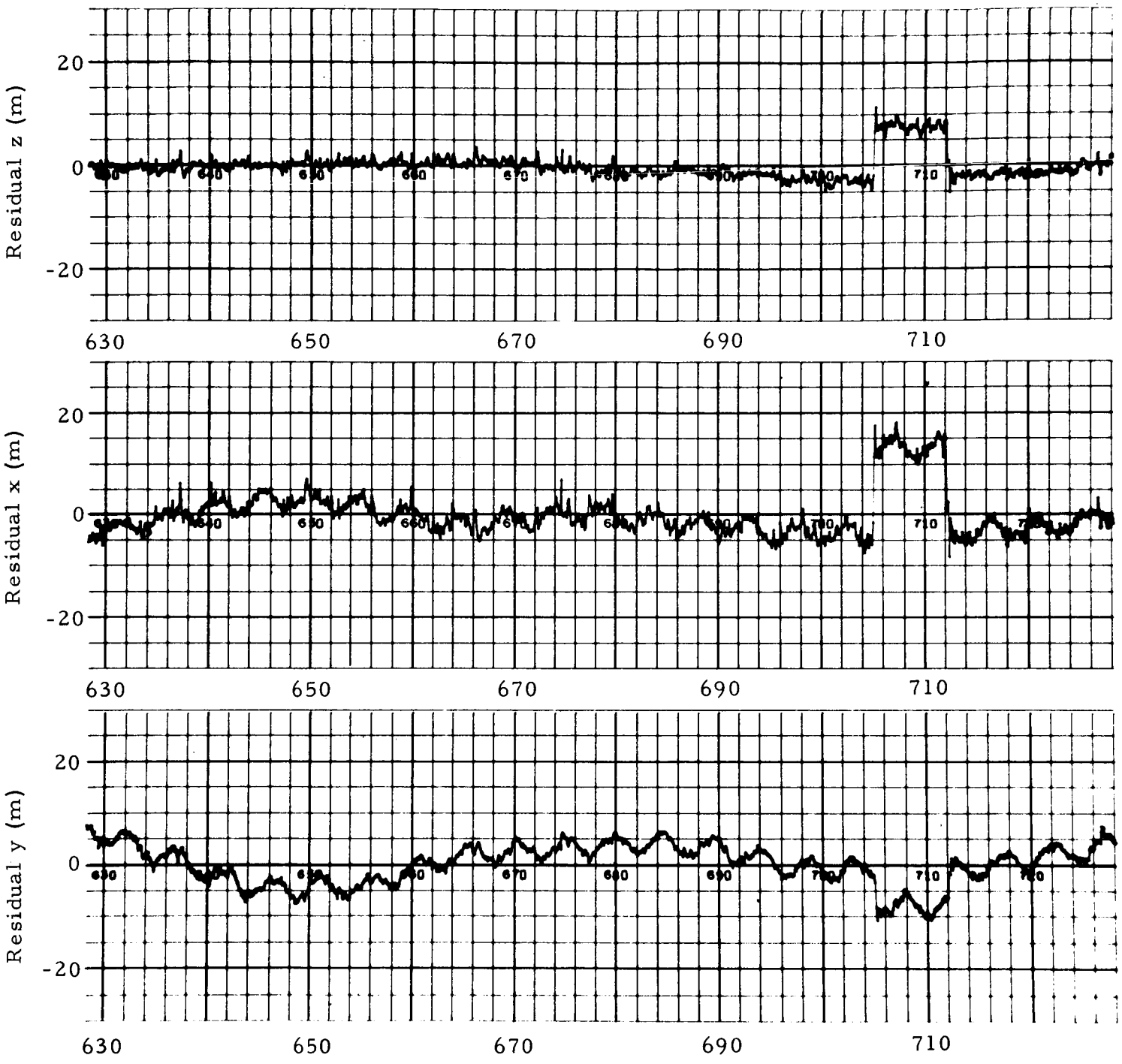

Fig. 11d - Example of Data Shift in Edited 0.1-sec Data (Detrended x y z Position Coordinates)

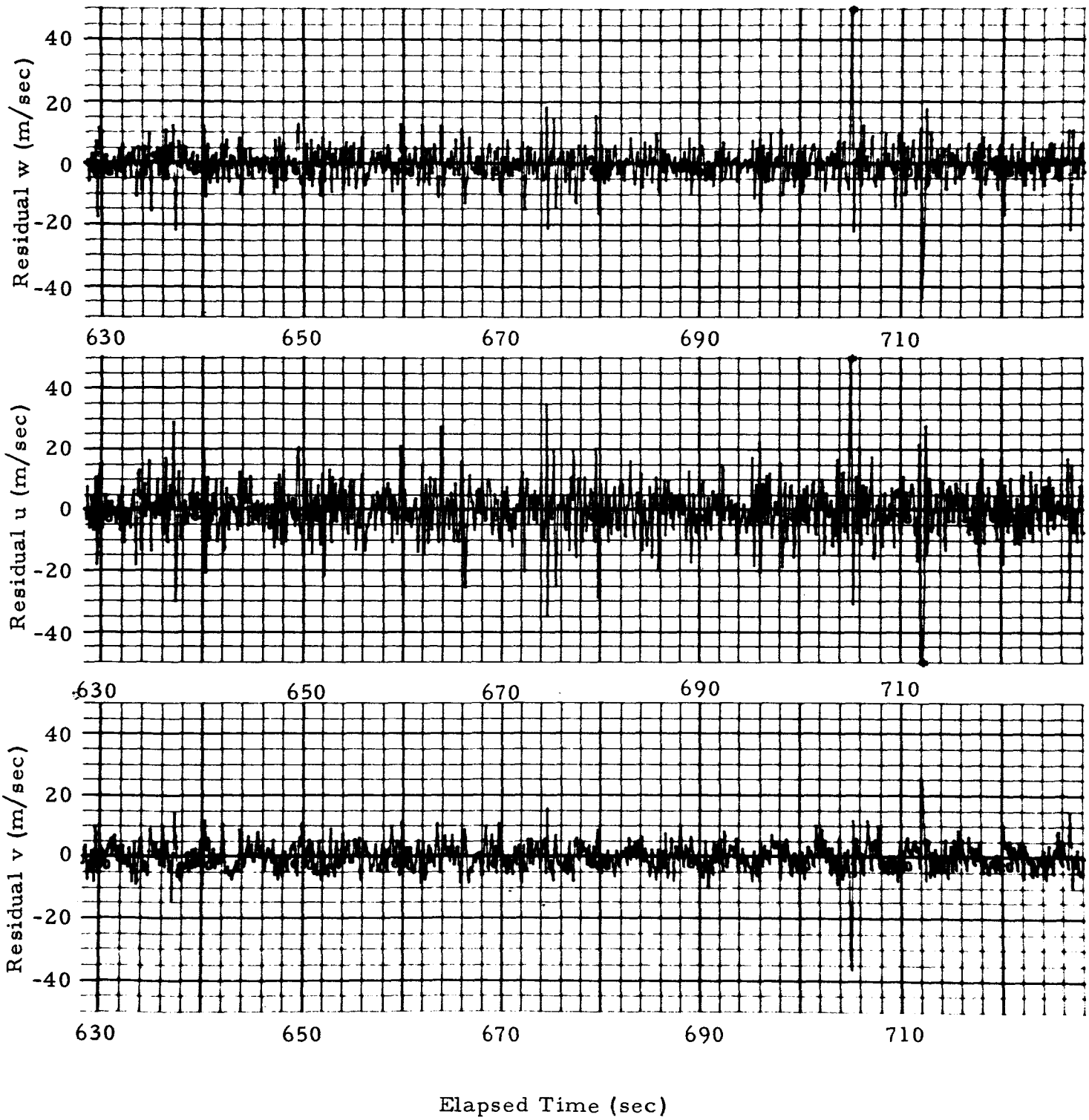

Fig. 11e - Example of Data Shift in Edited 0.1-sec Data
(Computed Velocity Residuals)

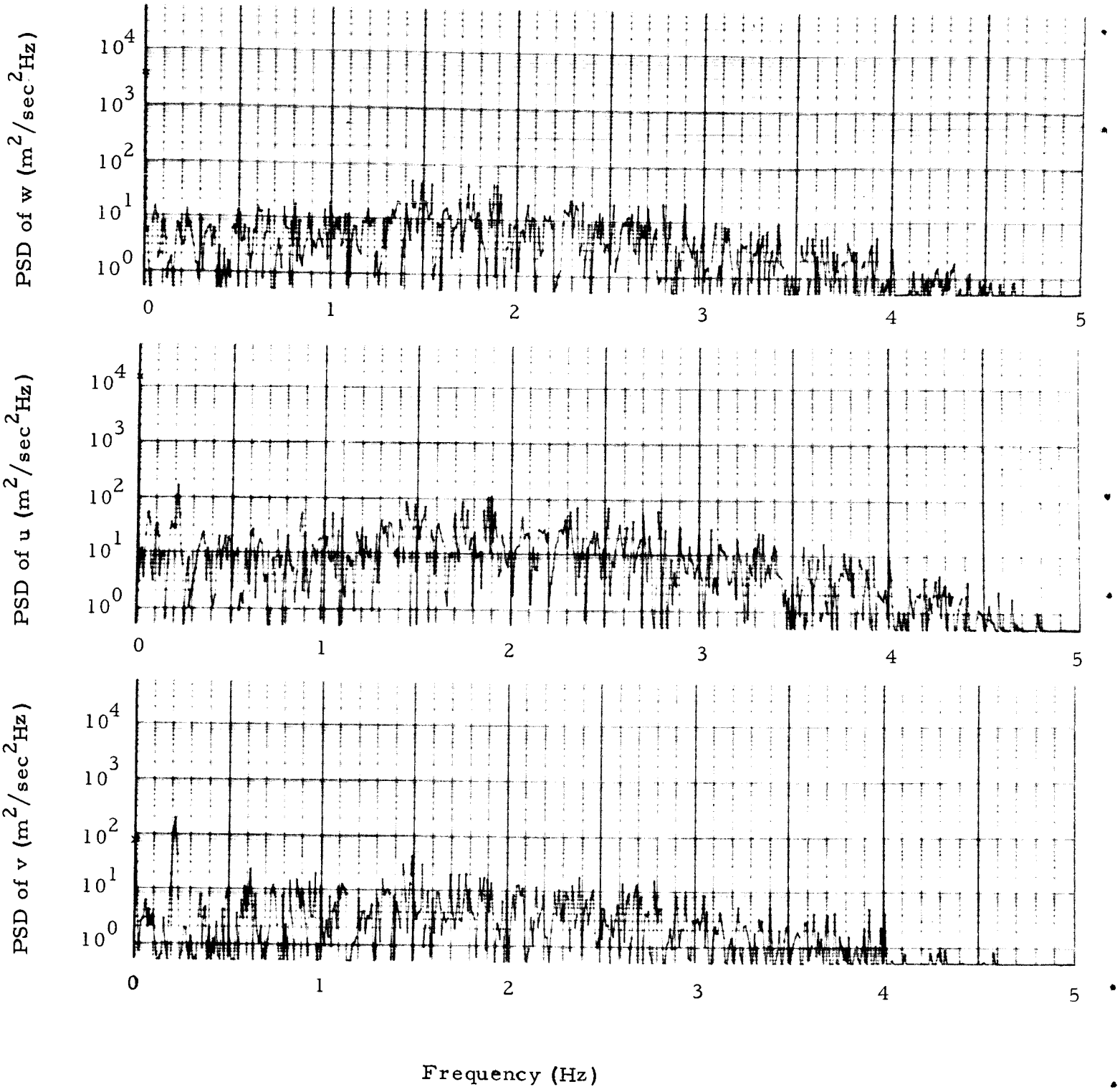

Fig. 11f - Example of Data Shift in Edited 0.1-sec Data
(Power Spectral Density of Velocity Components)

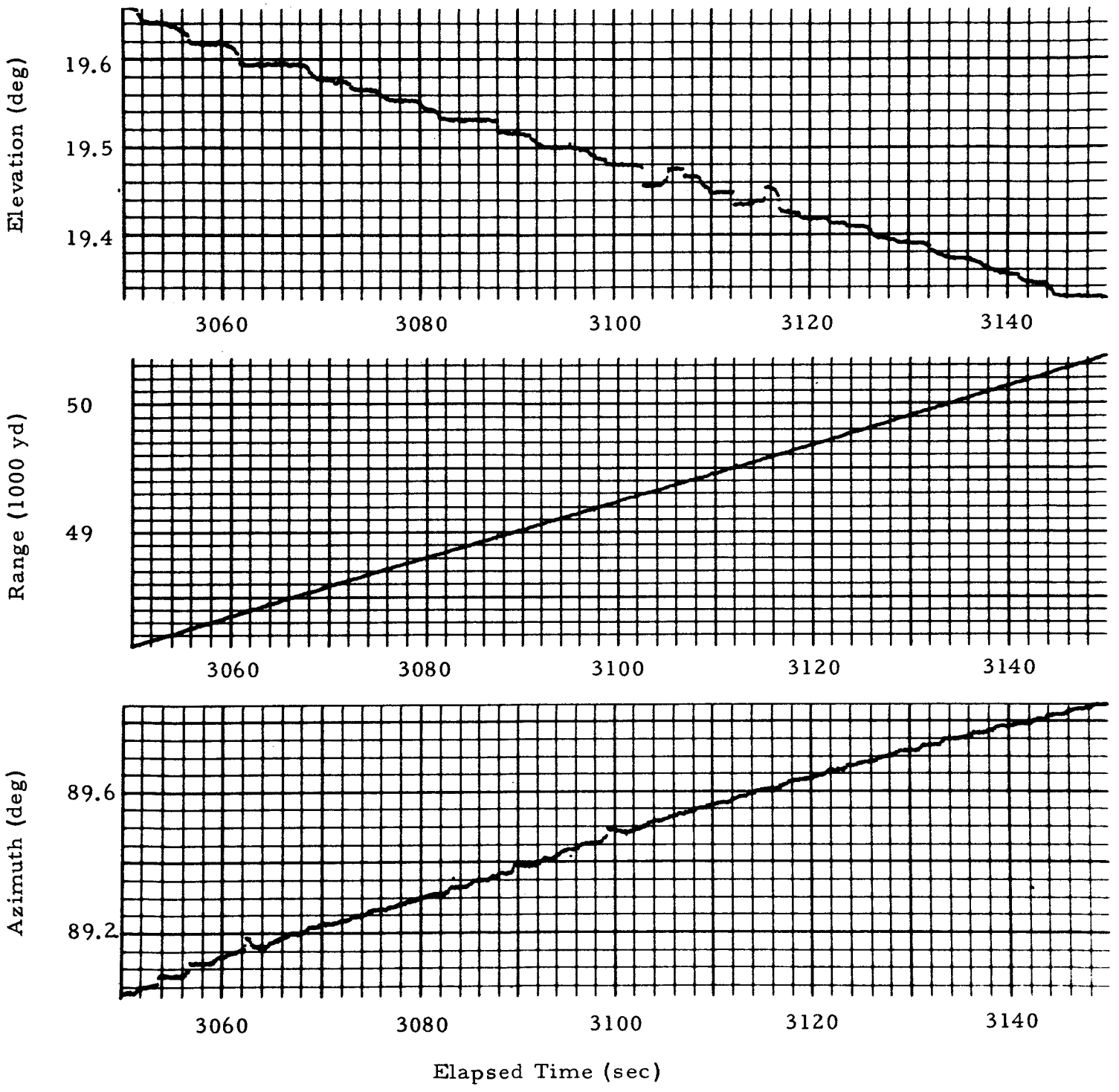

Fig. 12a - Example of Low Radar Response
(TAER Measurements)

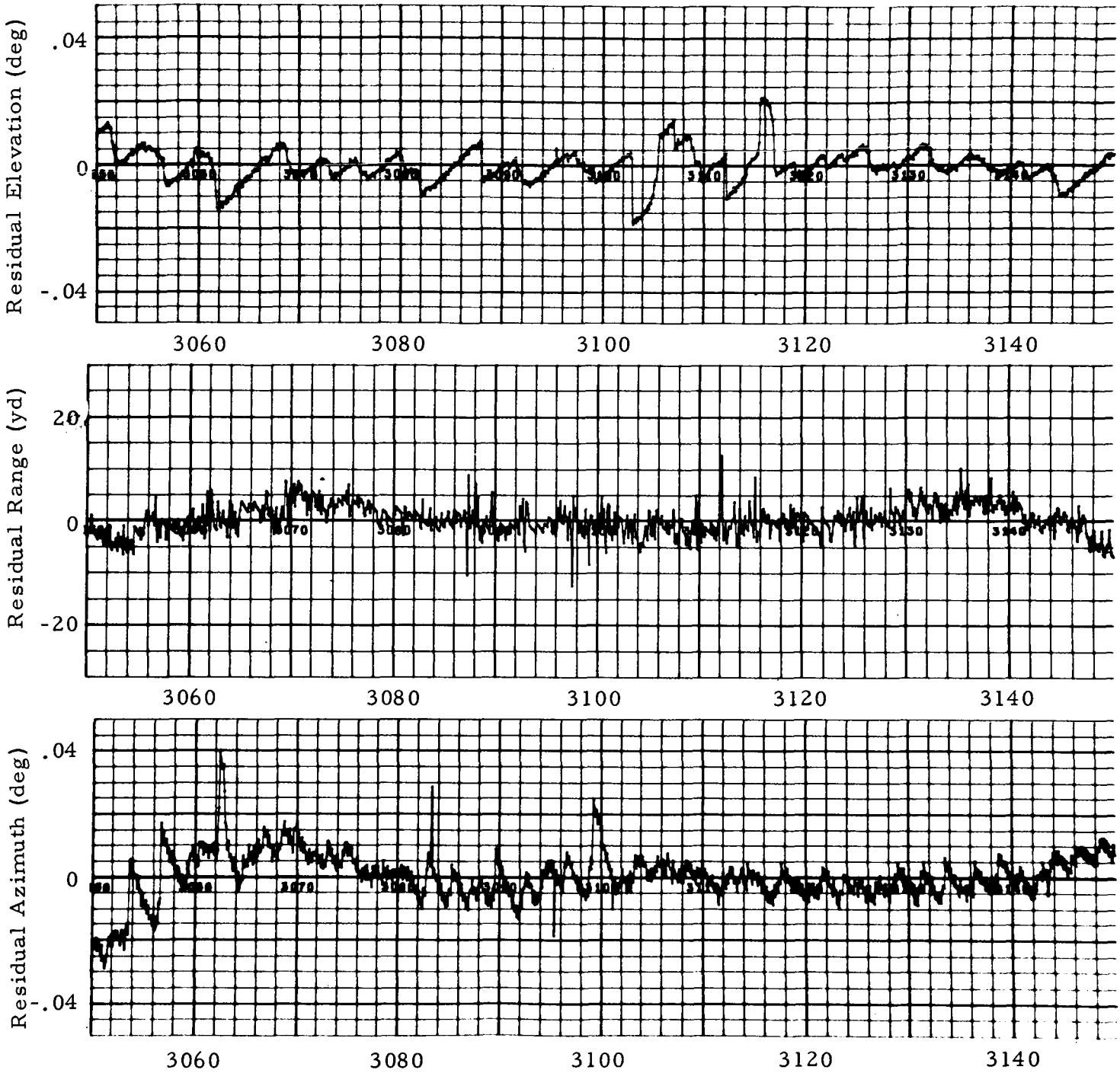

Fig. 12b - Example of Low Radar Response
(Detrended TAER Measurements)

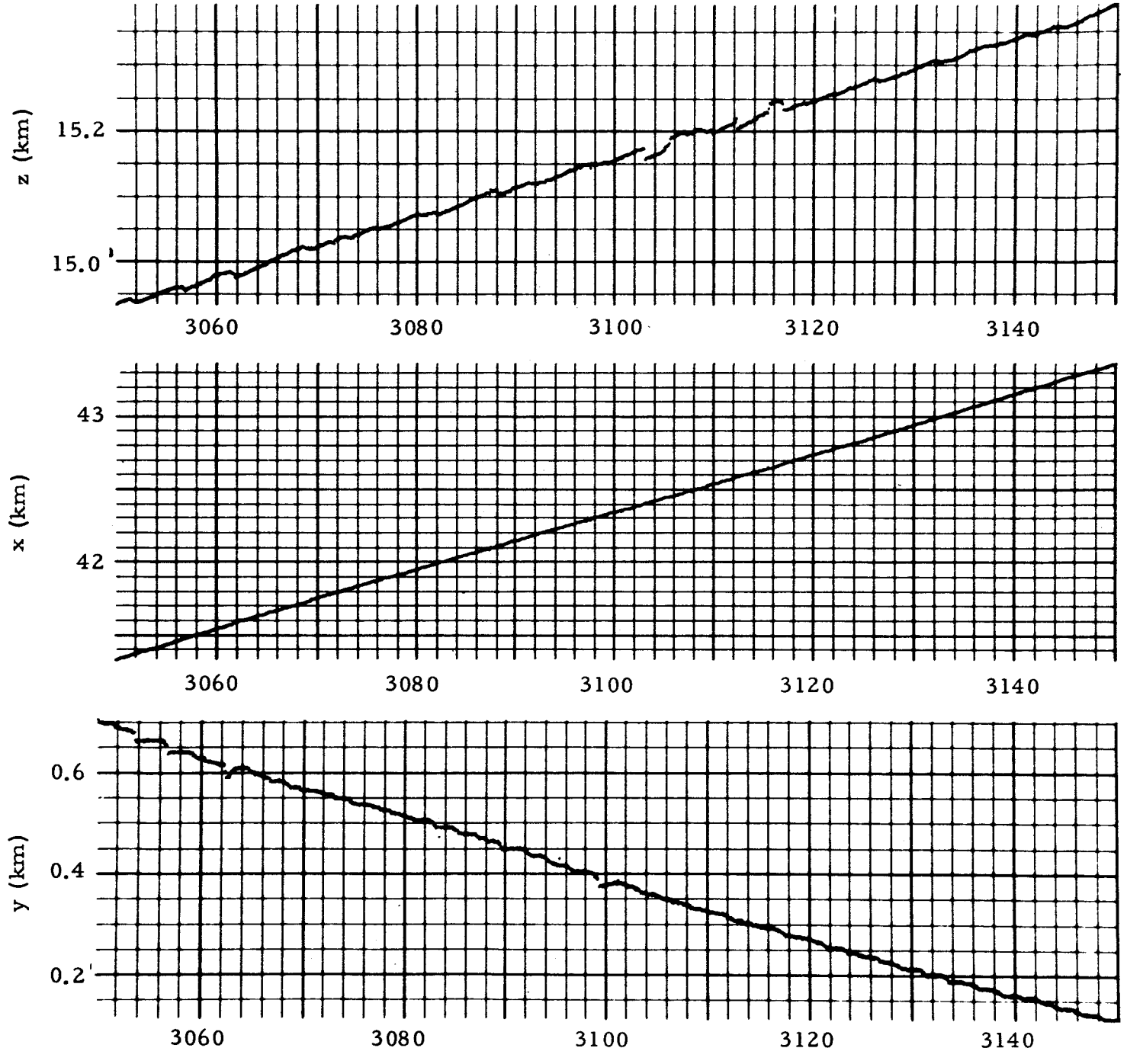

Fig. 12c - Example of Low Radar Response
(Computed x y z Position Coordinates)

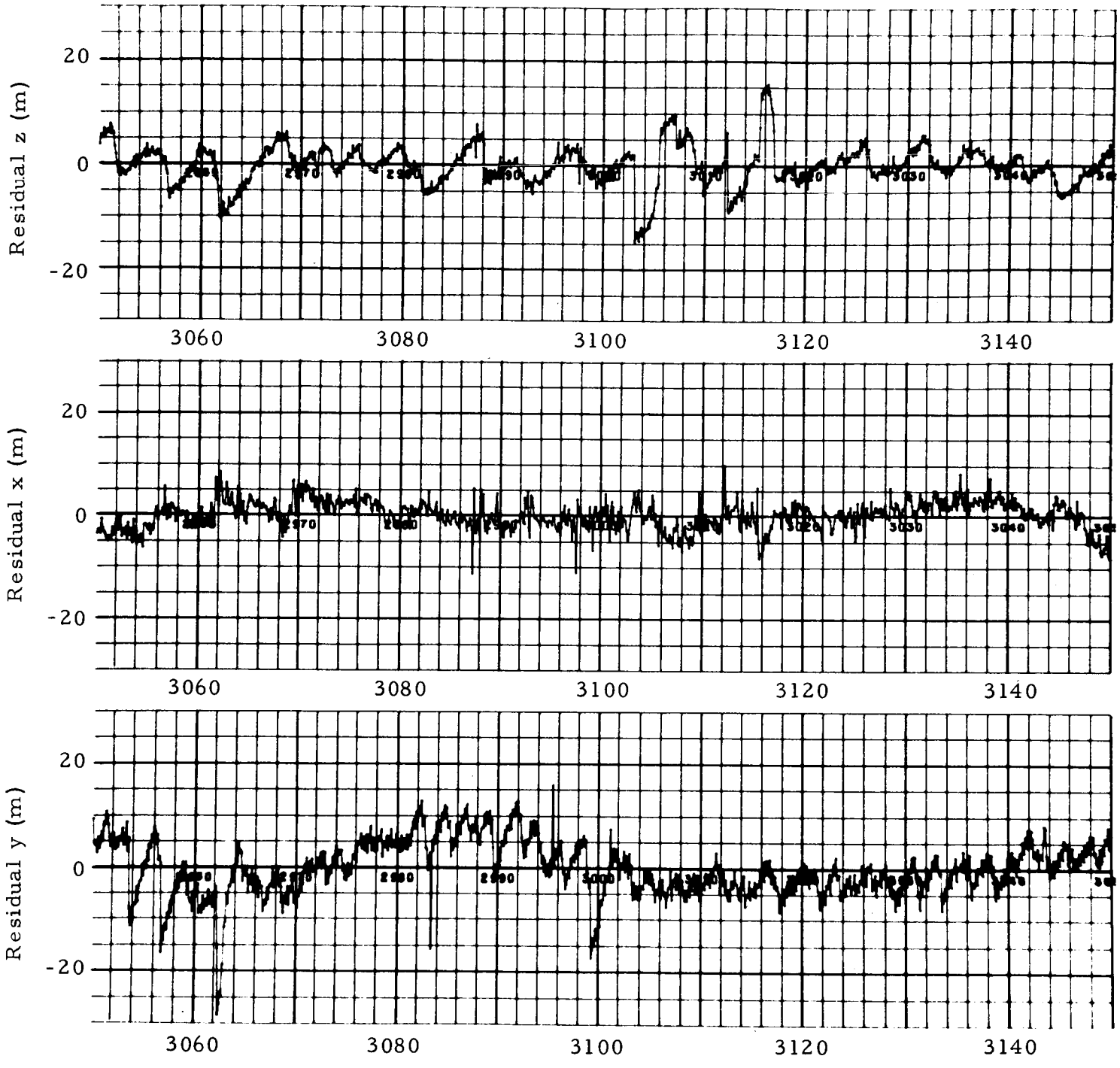

Fig. 12d - Example of Low Radar Response
(Detrended xyz Position Coordinates)

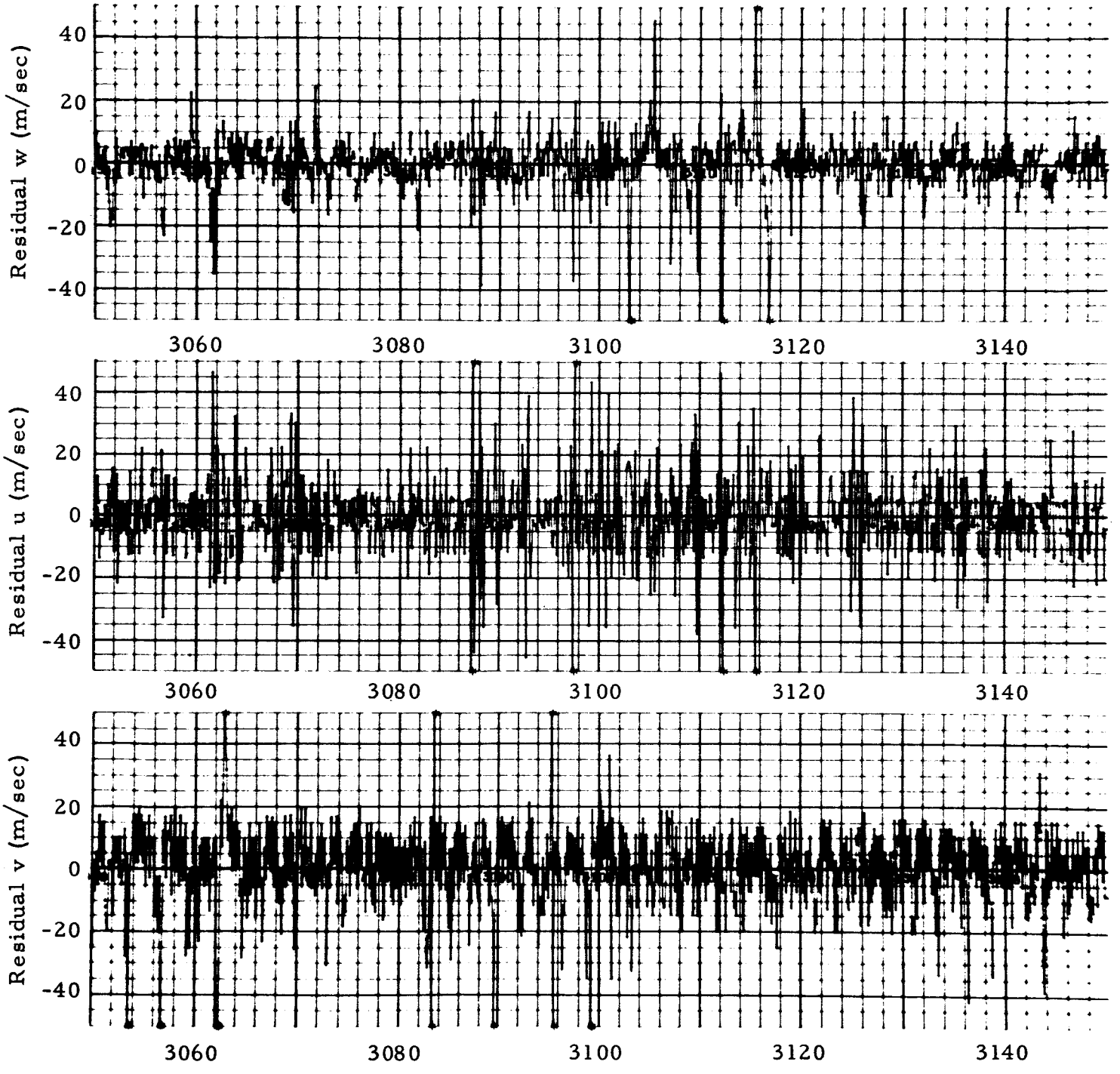

Fig. 12e - Example of Low Radar Response
(Computed Velocity Residuals)

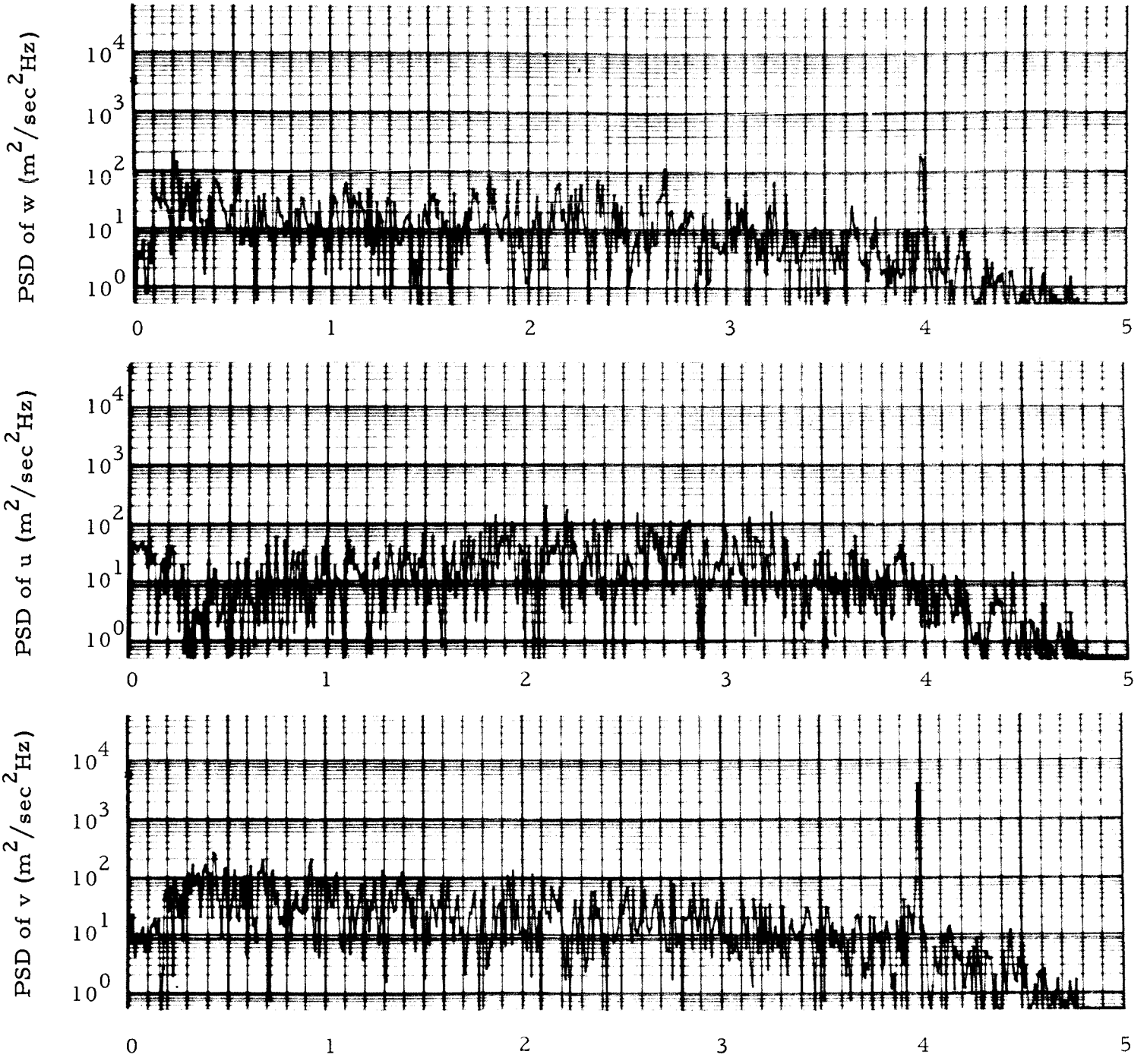

Fig. 12f - Example of Low Radar Response (Power Spectral Density of Velocity Components)

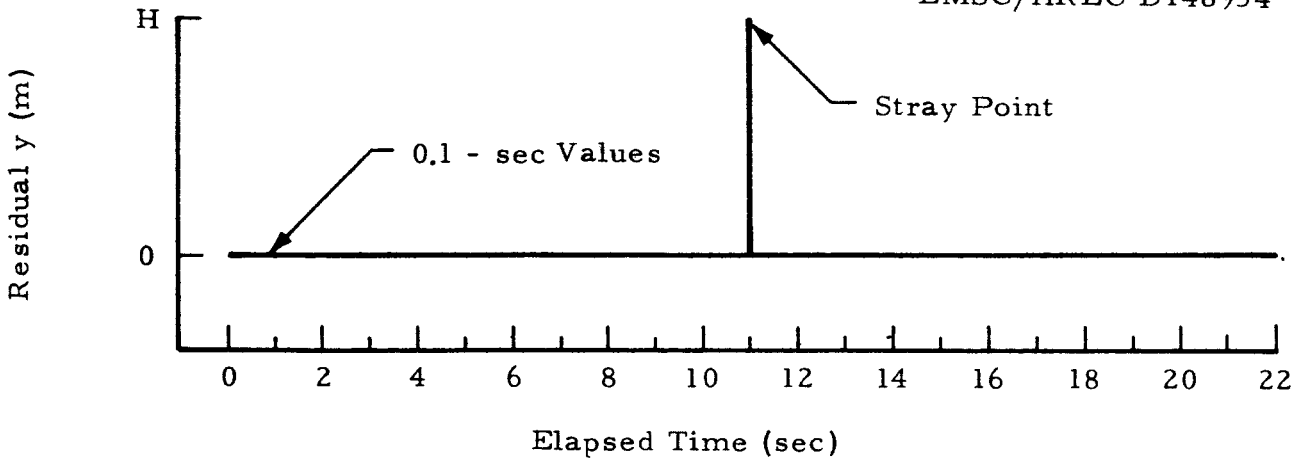

(a) Detrended 0.1 - sec y Values vs. Time

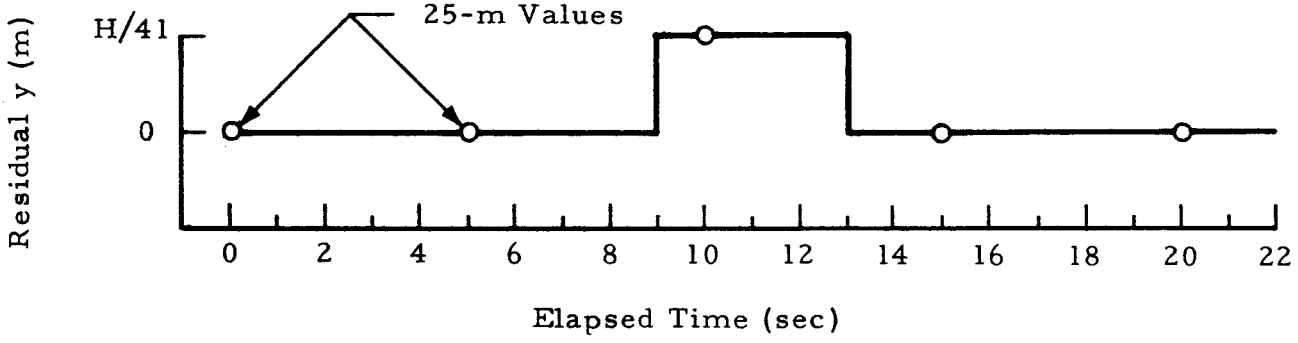

(b) Effect of 41-Point Moving Average on (a)

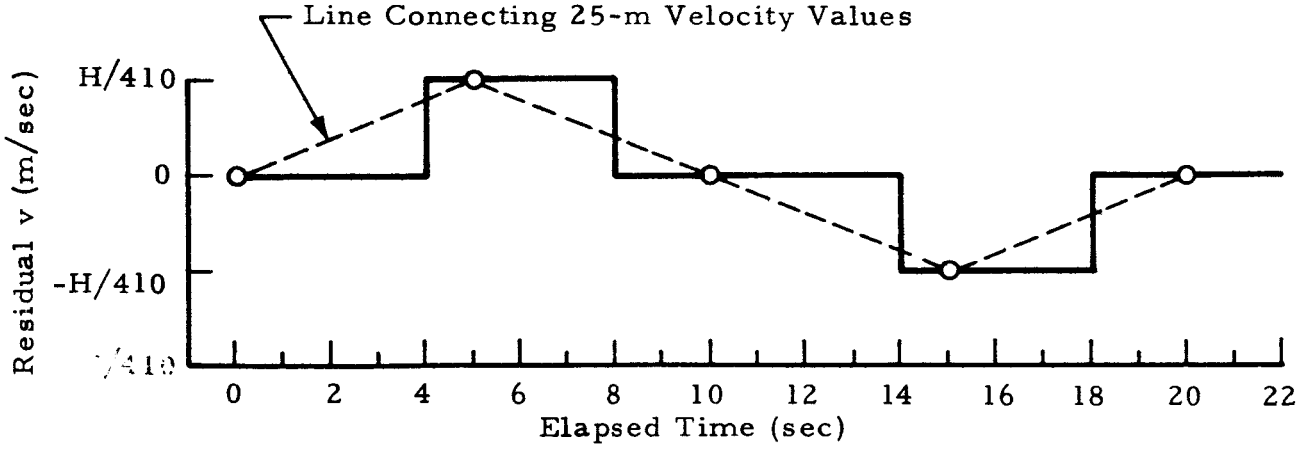

(c) Velocity Derived from 50-m (10-sec) Moving Centered Differences of (b)

Fig. 13 - Illustration of the Effect of One Stray 0.1-sec Position Value on Computed 25-m Wind Component Values

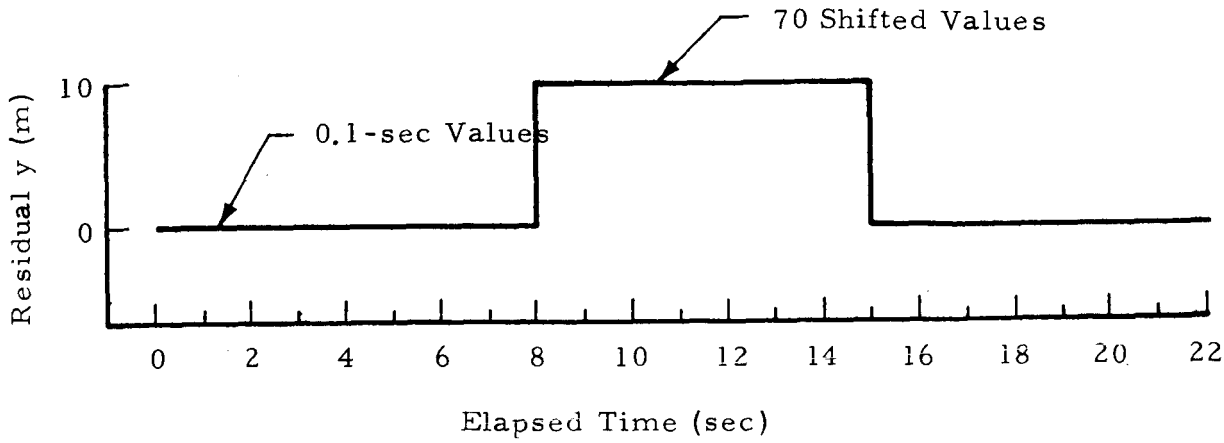

(a) Detrended 0.1-sec y Values vs. Time

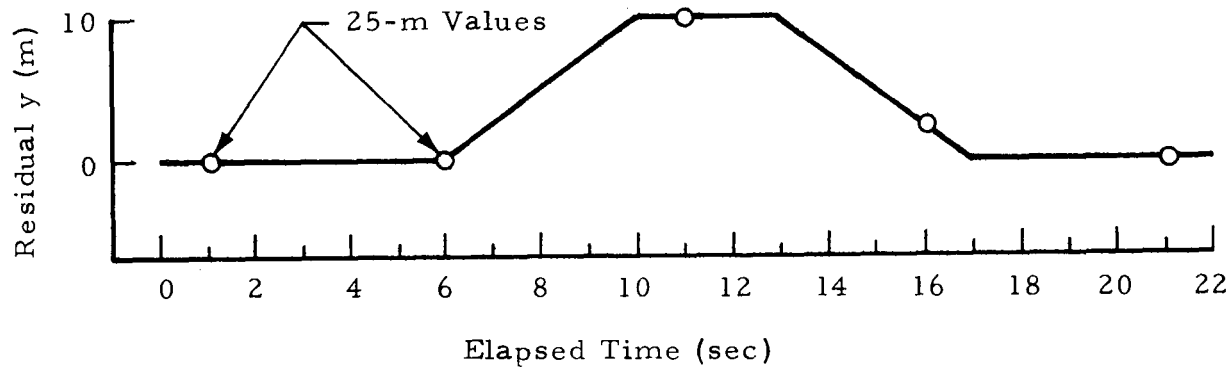

(b) Effect of 41-Point Moving Average on (a)

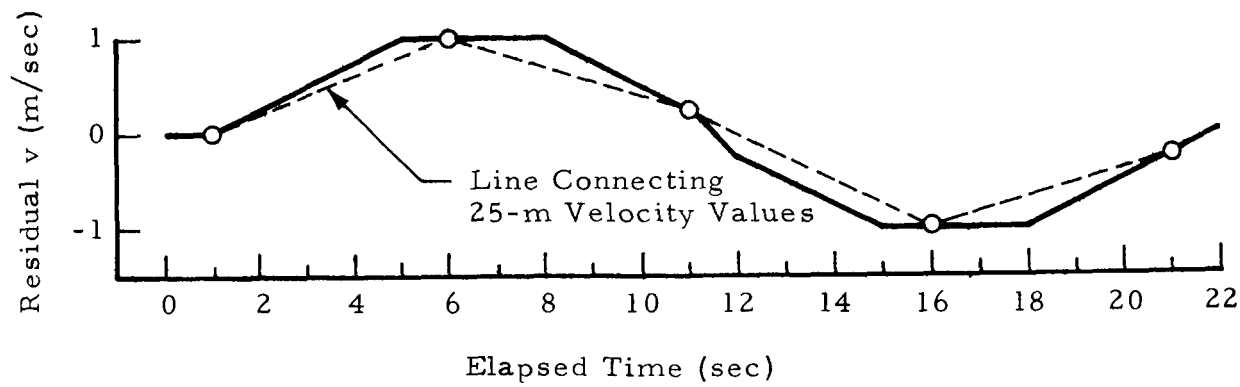

(c) Velocity Derived From 50-m (10-sec) Moving Centered Differences of (b)

Fig. 14 - Illustration of the Effect of a Data Shift on Computed 25-m Wind Component Values

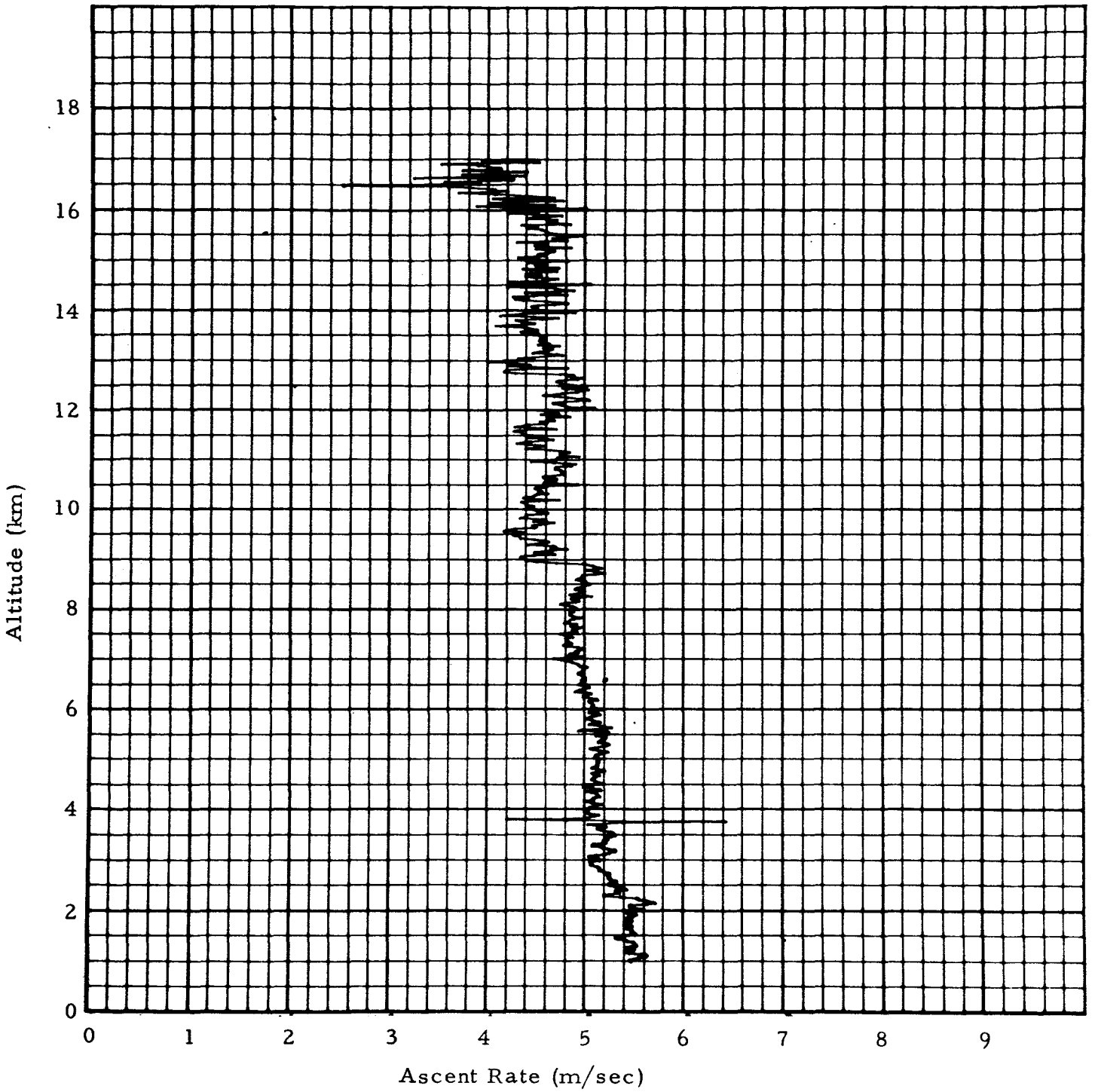

Fig. 15 - Ascent-Rate Profile Computed from the Sequence of TAER Measurements from which Figures 7a, 9a and 11a were Selected

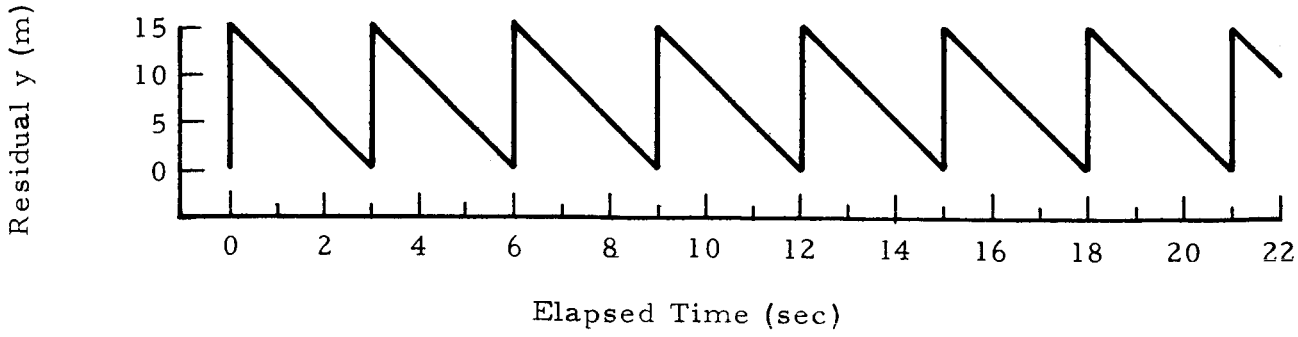

(a) Detrended 0.1-sec y Values vs. Time

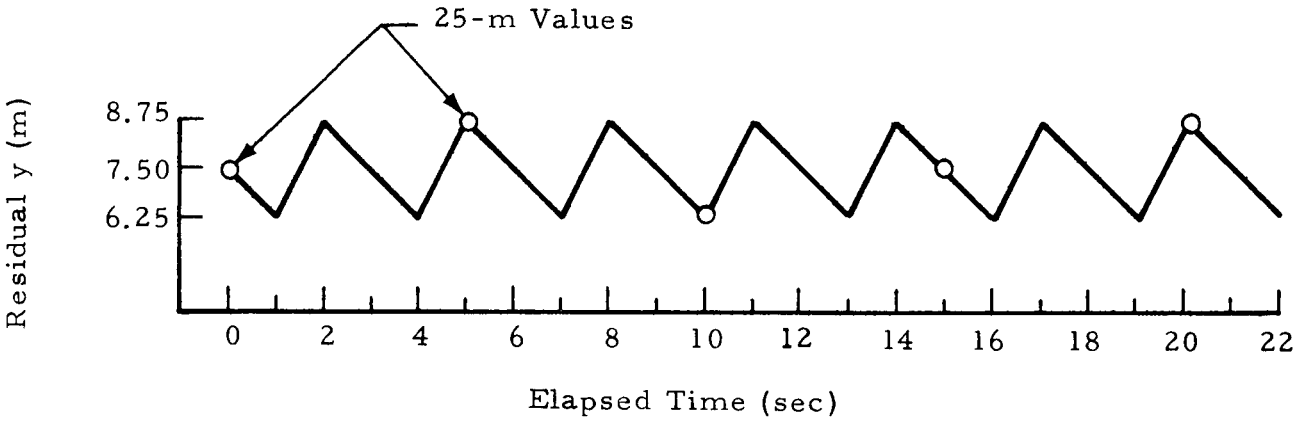

(b) Effect of 41-Point Moving Average on (a)

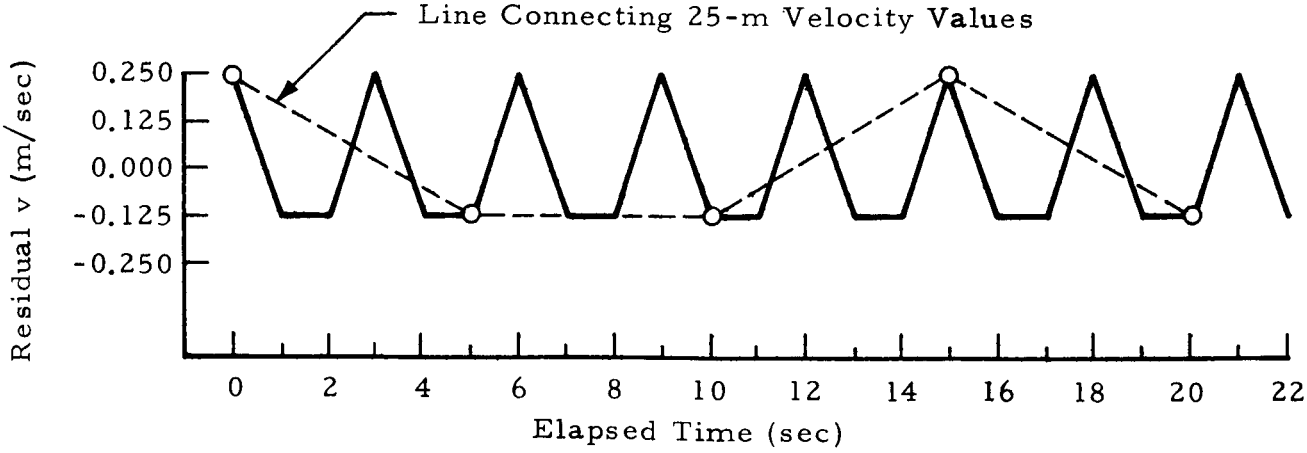

(c) Velocity Derived from 50-m (10-sec) Moving Centered Differences of (b)

Fig. 16 - Illustration of the Effect of a 3-sec Radar Response Lag on Computed 25-m Wind Component Values

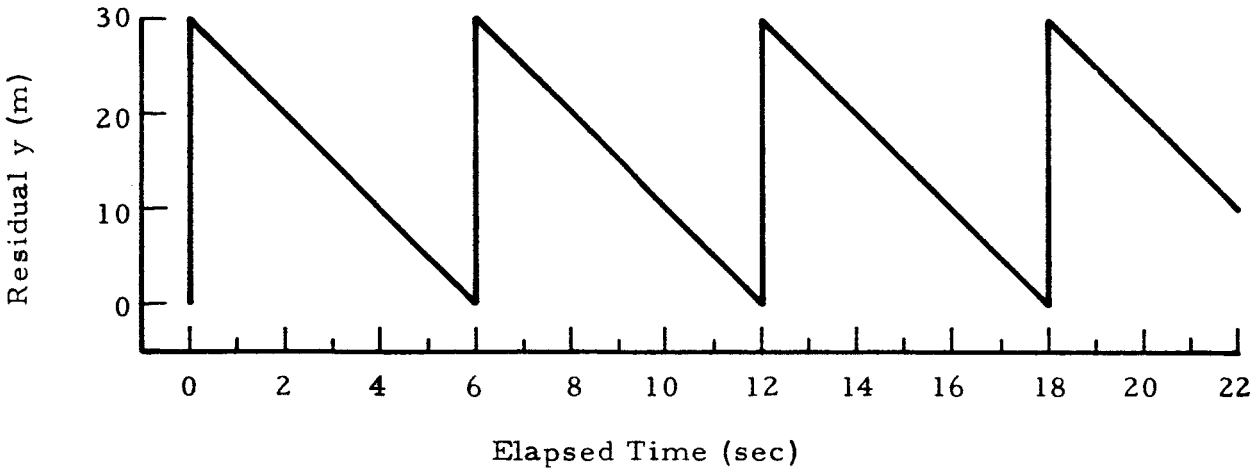

(a) Detrended 0.1-sec y Values vs. Time

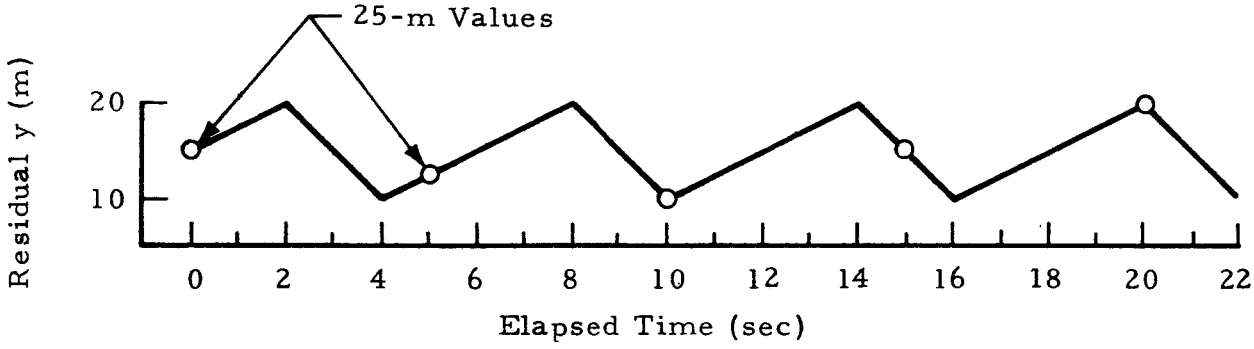

(b) Effect of 41-Point Moving Average on (a)

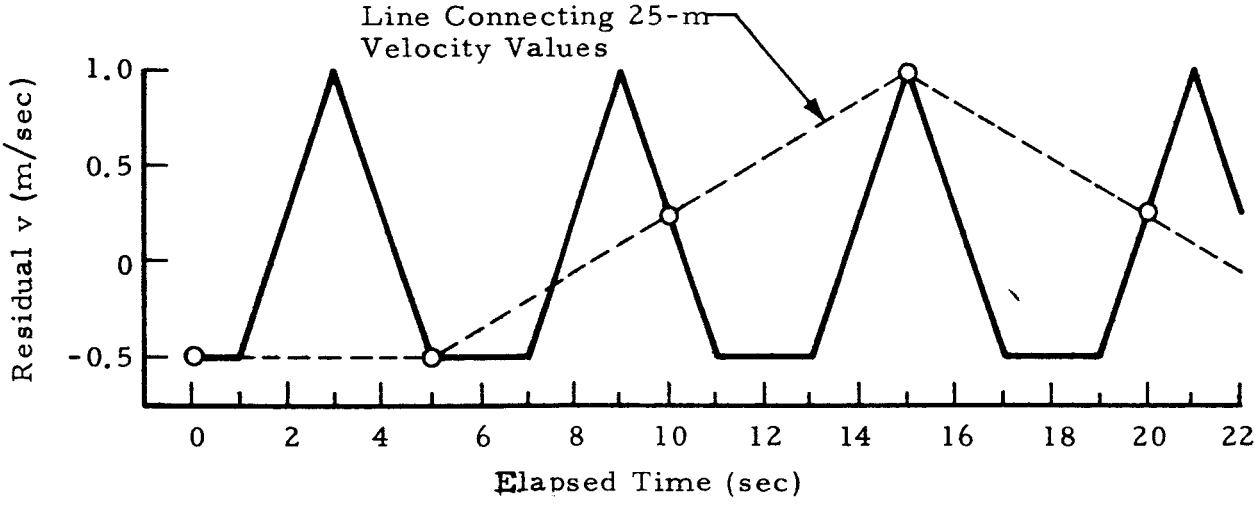

(c) Velocity Derived from 50-m (10-sec) Moving Centered Differences of (b)

Fig. 17 - Illustration of the Effect of a 6-sec Radar Response Lag on Computed 25-m Wind Component Values

MSFC—RSA, Ala